Reply to the Editor

We would like to thank the editor for his efforts to improve the manuscript. We address his general comments below. In the following, editor's comments are given in bold, author's responses in plain text. Suggested new text is quoted in italics.

General Comments

G1/ I recommend the paper be once more thoroughly checked by a native English speaker

The manuscript has now been corrected by a professional translation and editing company

G2/ Large parts of the result section are very descriptive and could be shortened.*

In compliance with this comment, we have shorterted the results section as much as we could.

G3/ Page1 / Line 16: The precision of the measurements have nothing to do with the compatibility goals, which are a maximal allowed bias. Please revise.

We have modified the text as suggested by the editor:

Thanks to the quality assurance strategy recommended by ICOS, the measurements uncertainties are within the World Meteorological Organisation compatibility goals for carbon dioxide (CO_2), methane (CH_4) and carbon monoxide (CO).

G4/ Figure 5: The differences shown in Figure 5 are relatively large (for hourly averages). Are these hourly averages representing the same data coverage for both instruments, or are the differences mainly due to different temporal coverage within one hour?

We agree with the editor that the differences are relatively large for hourly average. As stated in the manuscript, the "significant deviations may come from various sources of uncertainty, such as different residence time in the sampling systems, water vapour correction, clock issues, or internal analyser uncertainties." The differences may also come from differences in the sequence of air sampling, as we use a multi level air sampling system. The hourly means are computed based on only 15 minutes from the hour. The sampling sequencers were synchronized but sometimes the synchronization drifted or was lost for various reasons. If the sequencers are not synchronized, the air samples sampled are not the same and that can introduce large differences. We focused on the afternoon to reduce short term variabilities and to reduce local effects. Nevertheless, there are afternoon situations were short term variabilities are important and they were not filtered out.

We modified the following sentence to clarify this point:

For such atmospheric conditions, any difference in the air sampling sequences or in the time lag between air sampling and measurement in the analyser cell has a significant influence

G5/ Page 9 / Lines 3-6: Is this needed here? If so, more discussion is needed

We believe that this is useful information. Ancillary data are used to perform the automatic flagging of the raw data from the analysers. We modified the text as below:

Sequence data are used to generate the ambient air and cylinders raw time series. Mole fractions raw data are flagged automatically using the ancillary data based on a set of parameters defined for each station and instrument.

G6/ Page 27, Lines 2-4: 'After a long global decrease since the 1980's, the CO decrease has declined for several years after reaching values below 2 ppm (Lowry et al., 2016, Zellweger et al. 2016).' Something is wrong here. Should it be ppb instead of ppm? Since when has the decrease declined? By how much? (Zellweger et al., 2016) is not an appropriate citation here; (Zellweger et al., 2009) would be better..

We agree with this comment. We corrected the sentence and citations to

After a global decrease since the end of the 1980s, CO decrease has declined for several years after reaching values below 0.2 ppm at European background sites MHD or JFJ (Lowry et al., 2016, Novelli et al., 2003; Zellweger et al., 2009).

G7/Section 3.3: Scale issues are discussed in this chapter, and it is concluded that the differences can be explained by the bias in the reference scales. If I understood correctly, all comparisons were made on the same calibration scales. Therefore, I would be careful to call this scale issues, since the differences are probably only due to the uncertainties in the mole fraction assignment during calibration, which leads to small biases of the standards.

Indeed, there is no calibration scale issue as both systems are using the same primary WMO scale (CO_2: WMO X2007 CH_4: WMO X2004A CO: WMO X2014A). The observed bias is related to the uncertainty on mole fraction assignment of the 2 different sets of working standards used independently by the station onsite analysers and the FMI's travelling instruments. These 2 sets of standards have been calibrated against the same WMO scale but using 2 different tertiary standards (FMI and LSCE) with 2 independent setups and associated data processing. The multiplicity of intermediary standards in the calibration chain increases uncertainties and may lead to bias in the 2 different sets of calibrations standards.

A misuse of "scale" instead of "calibration standards" in the text leads to this confusion.

We modified the following sentence to clarify this point:

Most of the differences in ambient air measurements can be explained by biases in the working standards. The instruments and the working standards (OPE and travelling standards) were calibrated against two different sets of tertiary standards, introducing biases in the measurements of the cylinders and of ambient air.

G8/ Font size in many figures might be too small to be readable in the final AMT paper.

We could make new plots with larger font size if needed

G9/ The term 'concentration' is widely used throughout the manuscript and mixed with other terms such as 'mole fraction' and 'mixing ratio'. Concentration in the context of GHG measurements is not correct and needs to be replaced by mole fraction or amount fraction (mixing ratio might also be acceptable).

We replaced concentration by mole fraction throughout the manuscript

Technical corrections:

T1: done

T2: done

T3: done

T4: done

T5: done

T6: done

T7: done

T8: done

T9: done

T10: done

T11: done

T12: We modified the sentence to: *Clusters 1, 2 and 3 are characterised by continental air masses (mostly from the south, east and north respectively)*

T13: done

T14: done

T15: done

T16: We modified the sentence to: *The standards mole fractions cover the unpolluted atmospheric range following ICOS Atmospheric Station specifications (Laurent, 2017).*

T17: done

T18: the scale references were corrected

T19: done

T20: done

T21: done

T22: done

T23: done

T24: done

T25: Title 3.2 was simplified to *Field long term repeatability*

T26: 'dried Picarro' and 'wet Picarro', and similar expressions were removed

T27: The sentence was changed to *The CO comparison was carried out for OPE-LGR and OPE-G2401 instruments and compared to the TI G2401: the average deviations exceeded the WMO/GAW component compatibility goal (±2 ppb).*

T28: done

T29: done

T30: done

T31: There are only 3 colours in the plots, the other colour being a mixture of red, green and blue for the part of the plots were the areas are common to the 3 colours

T32: The text was modified as suggested

T33: done

T34: Reference to JFJ was removed

T35: done

T36: ERIC (European Research Infrastructure Consortium) was removed from the sentence

Continuous atmospheric CO_2, CH_4 and CO measurements at the Observatoire Pérenne de l'Environnement (OPE) station in France from 2011 to 2018

Sébastien Conil[1], Julie Helle[2], Laurent Langrene[1], Olivier Laurent[2], Marc Delmotte[2], Michel Ramonet[2]

[1]DRD/OPE ,Andra, Bure,55290, FRANCE
[2] Laboratoire des Sciences du Climat et de l'Environnement (LSCE/IPSL), UMR CEA-CNRS-UVSQ, Gif-sur-Yvette, France

Correspondence to: Sébastien Conil (sebastien.conil@andra.fr)

Abstract.

Abstract. Located in North-East France, the Observatoire Pérenne de l'Environnement (OPE) station was built during the Integrated Carbon Observation System (ICOS) Demonstration Experiment to monitor the atmospheric concentration of greenhouse gases mole fraction. Its continental rural background setting fills the gaps between oceanic or mountain stations and urban stations within the ICOS network. Continuous measurements of several greenhouse gases using high precision spectrometers started in 2011 on a tall tower with three sampling inlets at 10m, 50m and 120m above the ground level (agl). The mMeasurements' quality is regularly assessed using several complementary approaches based on reference high pressure cylinders, travelling instruments audits using travelling instruments and sets of travelling cylinders (so-called "cucumber" intercomparison program). Thanks to the quality assurance strategy recommended by ICOS, the precision of the measurement s uncertainties is are within the World Meteorological Organisation compatibility goals for carbon dioxide (CO_2), methane (CH_4) and carbon monoxide (CO). The time series of mixing ratios time series from 2011 to end of 2018 are used to analyse trends and diurnal and seasonal cycles. The CO_2 and CH_4 annual growth rates are respectively 2.4 ppm/year and 8.8 ppb/year, respectively, for the measurements at 120m agl over the investigated period. However, no significant trends has've been recorded for the CO mixing ratios. The afternoon mean residuals (defined as the differences between midday observations and a smooth fitted curve) of these three compounds are significantly stronger during the cold period when inter-species correlations are high, compared to the warm period. The variabilities of residuals show a close link with the air mass back-trajectories.

1 Introduction

Since the beginning of the industrial era, the atmospheric mole fractions concentration of long lived greenhouse gases (GHGs) has've been rising. Increases of in surface emissions, mostly from human activities, are responsible for this atmospheric GHG's build up. For carbon dioxide (CO_2), the largest climate change contributor, only around half of the additional anthropogenic emissions are retained in the atmosphere, with the remaining 50% being pumped absorbed out by the ocean and the land

Mis en forme : Exposant

Mis en forme : Indice

Mis en forme : Indice

ecosystems (Le Quéré et al., 2018). ~~Regarding~~ For ~~the~~ methane (CH_4) the last ~~10~~ ten years are characteri~~s~~zed by high growth rates at many observation sites, following a period of stable mole fraction~~concentration~~s from 2000 to 2007 (Nisbet et al., 2019; Turner et al., 2019). Monitoring the ~~atmospheric~~ amount fractions ~~concentrations~~ of th~~e~~o~~s~~e GHG~~'s~~ is of primary importance for the long-term climate monitoring but also for the assessment of surface fluxes ~~assessment~~. ~~Remote and mountain atmospheric measurements, because they are performed far from anthropogenic sources and/or are located in the free troposphere,~~ Remote and mountain atmospheric measurements are ~~necessary~~ needed to assess ~~the~~ background mole fraction~~concentration~~s because they are performed far from anthropogenic sources and/or are located in the free troposphere. Such « global scale » data are of great value ~~to~~ for monitoring the global atmospheric GHG build-up ~~but also~~and estimating ~~to estimate~~ global scale fluxes. However, they are not designed to capture the regional-scale signals necessary to assess local to regional scale fluxes. The specific purpose of the European Integrated Carbon Observation System (ICOS) ~~precisely aims a~~is ~~t~~ to establish and maintain a dense European GHG observations network to monitor long-term changes, assess the carbon cycle and track carbon and GHG fluxes. ~~Atmospheric i~~Inverse atmospheric methods combining tall tower network measurements and transport models are ~~great~~ important tools ~~to~~ for assessing ~~the~~ surface GHG fluxes exchanged with the biosphere and oceans, and ~~to~~ estimateing the anthropogenic emissions (Broquet et al., 2013; ~~;~~Kountouris et al., 2018). They also offer independent ways to improve the bottom-up emissions inventories required by the international agreement under the United Nations Framework Convention on Climate Change ~~UNFCC~~ (Bergamaschi et al., 2018; Leip et al., 2018; Peters et al., 2017).

ICOS was established as a European strategic research infrastructure which will provide the high precision observations needed to quantify the greenhouse gas balance of Europe and adjacent regions. It is now a ~~distributed~~ widespread infrastructure ~~composed~~ made up of three integrated networks measuring GHGs in the atmosphere, over the ocean and at the ecosystem level. Each network is coordinated by a thematic center that performs centrali~~s~~zed data processing. One of the key focuses of ICOS is to provide standardi~~z~~sed and automated high-precision measurements, which is achieved by using common measurement protocols and standardi~~z~~sed instrumentations. In the atmospheric monitoring network, ICOS targets the World Meteorological Organization (WMO) / Global Atmosphere Watch (GAW) compatibility goal (WMO, 2018) within its own network as well as with other international networks. During the preparatory phase from 2008-2013 a demonstration network and new stations were set up with harmoni~~s~~zed specifications (Laurent et al ; 2017). The Atmospheric Thematic Center (ATC) performs several metrological tests on the analysers ~~as well as~~and provides technical support and training regarding ~~any~~ all aspects of the in situ GHG measurements (Yver Kwok et al., 2015). The ATC is also responsible ~~of~~ for the near real time post processing of the measurements (Hazan, et al., 2016).

The OPE station was established ~~as~~ under a close collaboration between the French national radioactive waste management agency (Andra) and the Laboratoire des Sciences du Climat et de l'Environnement (LSCE) ~~in the frameworkas~~ part of the demonstration experiment during 2010 and 2011 ~~following~~ in accordance with~~the~~ ICOS atmospheric station specifications. It is a continental regional background station contributing to the ~~actual~~ network by bridging the gap between remote ~~global/mountain~~ station~~s~~ like Mace Head (MHD) or Jungfraujoch (JFJ), and urban stations like Saclay or Heidelberg. The

Mis en forme : Indice

Mis en forme : Anglais (États-Unis)

potential of ICOS continuous measurements of CO_2 dry air mole fraction to improve Net Ecosystem Exchange estimates at the mesoscale across Europe wash~~has been~~ evaluated in Kadygrov et al. (2015). Pison et al. (2018) addressed the potential of the ~~actual~~ current ICOS European network for estimating methane emissions at the French national scale~~the methane emission estimation at the French national scale~~.

The main objectives of this paper are to describe the OPE monitoring station and~~,~~ the continuous GHG measurements system, to present its performance characteristic and to draw ~~some~~ results from the first ~~8~~eight years of continuous operations.

2 Site description and GHG measurements system

2.1 Site location

The OPE atmospheric station (48.5625°N, 5.50575°E WGS84, 395 m asl) is located on the eastern edge of the Paris Basin in the n~~N~~orth~~- E~~east part of France, western Europe, as shown on Figure 1~~Figure 1~~. The landscape consists of undulatinged eroded limestone plateaus~~x~~ dissected by a few SE-NW valleys (60 to 80m). The station is on top of the surrounding hills in a rural area with large crop fields, some pastures and forest patches. ~~The dominating land cover types~~ A~~a~~ccording to Corine Land Cover 2012, the dominant land cover types in the 25 / 100 km surrounding~~s~~ area are Arable land/crops: 39% /44%, Pastures : 14% /18%, Forest : 44% /34%. Based on GEOFLA database from Institut national de l'information géographique et forestière (IGN), t~~T~~he mean population density within a 25 / 100km radius from the station ~~based on GEOFLA database from Institut national de l'information géographique et forestière (IGN)~~ is ~~are~~ 26 / 64 (inhab.km^{-2}). The closest small towns are Delouze with 130 people located 1 km ~~at~~ to the ~~SE~~ south-east and Houdelaincourt with 300 people located 2km ~~at~~ to the ~~SW~~south-west. The closest cities are Saint Dizier (45,~~-~~000 inhabitants) located 40km away ~~at~~ to the w~~W~~est, Bar Le Duc (35, 000 inhab.) 30km at the ~~NW~~north-west, Toul (25,~~-~~000 inhab.) 30km ~~at~~ to the e~~E~~ast and Nancy (450,~~-~~000 inhab.) 50km ~~at~~ to the east~~E~~. ~~The major road w~~With 20 000 cars/day, the major road is located 15km to the ~~N~~north (RN4). The station includes a 120m tall tower and two portable and fully equipped modular buildings ~~fully equipped i~~on a 2ha fenced area. The station infrastructure~~s~~ w~~ere~~as built in 2009 and 2010 and the measurements systems started in 2011.

The OPE station is designed to host a complete set of in situ measurements of meteorological parameters, trace gases (CO_2, CH_4, N_2O, CO, O_3, NO_x, SO_2) and particle~~s~~ parameters(size distribution, absorption and diffusion coefficients, number and mass, chemical composition, radioactivity). The station is part of the French aerosol in situ network contributing to ACTRIS and AERONET program. It is part of the IRSN (Institut de Radioprotection et de Sûreté Nucléaire) network for ~~the~~ ambient air radioactivity monitoring. The station ~~is~~ also contribute~~s~~i~~ng~~ to the ~~french~~French air quality monitoring network and to the European Monitoring and Evaluation Program.

Figure 1: Geographical location of the OPE atmospheric station (left ~~panel~~) and aerial photograph illustrating the landscape surrounding the station (right ~~panel~~).

2.2 Local meteorology and air mass~~es~~ trajectories

~~The~~ L~~l~~ocal meteorology is monitored using three sets of meteorological sensors located at the three measurement levels on the tower (10m, 50m and 120m agl). Standard meteorological parameters, Temperature, Relative Humidity, Pressure and Wind Speed and Direction, are monitored in compliance with ~~the~~ ICOS Atmospheric Station specifications. Minute averaged data are logged and used to produce hourly mean fields. In addition there is a ground based weather station operated by Meteo France, the French national weather service providing hourly mean data in compliance with ~~the~~ World Meteorological Organization specifications.

The mean annual temperature ~~over the period~~between ~~-~~2011~~-~~ and 2018 was~~is~~ ~~around~~ 10.5°C. The minimum temperature was -15,~~,~~2°C and the maximum temperature was 36.4°C. The cumulated annual precipitation~~s~~ ~~are~~ was ~~on average~~ 829mm on average. Two local wind regimes are predominant, a south~~/-~~westerly regime and an east~~erly/-~~north easterly regime.

~~96h back trajectories were computed for the OPE station top level (120m) using the NCEP reanalysis fields and HYSPLIT model every 6 hours. As we focus on the afternoon mean residuals, we use only back-trajectories reaching the OPE station at 12:00 UTC. The clustering tools from HYSPLIT was used to determine the main air masses type reaching the station. Six clusters were defined as shown on the Figure 2. This figure shows the frequency of trajectories for each cluster passing through the corresponding grid point and reaching the OPE station at 12:00 UTC. Clusters 1 to 3 are characterized by continental air masses type. Cluster 4 is dominated by slow moving trajectories from the western part. Cluster 5 and 6 are dominated by western marine trajectories.~~

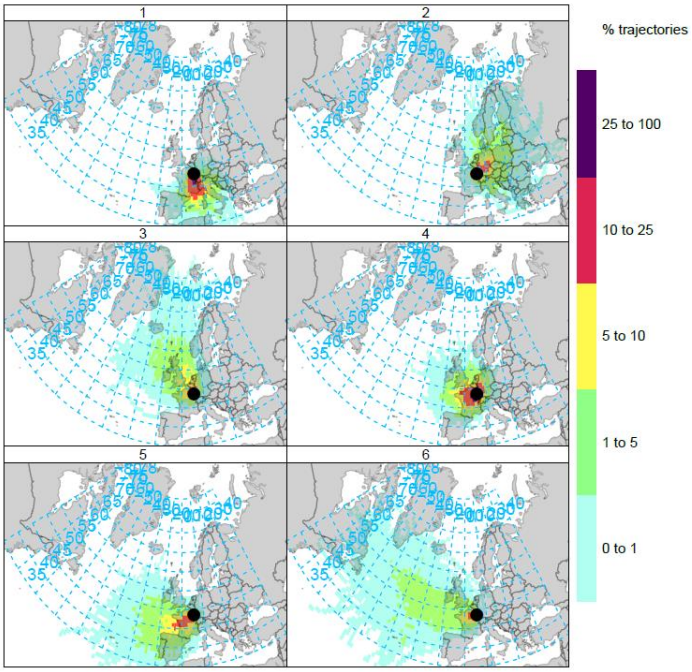

Figure 2: 96hours back-trajectory frequencies reaching the OPE station top level for each of the 6six clusters identified using the HYSPLIT tools and the NCEP reanalysis for the period 2011-2018.

96h back trajectories were computed for the OPE station top level (120m) using the National Centers for Environmental Prediction (NCEP) reanalysis fields and the HYSPLIT model every 6 hours. As we focus on the afternoon mean residuals (defined as the differences between midday observations and a smooth fitted curve), we only use back-trajectories reaching the OPE station at 12:00 UTC. The clustering tools from HYSPLIT were used to determine the main types of air mass reaching the station. Based on the total spatial variance (TSV) metric, describing the sum of the within cluster variance, the optimal number of clusters was six (lowest number with a small TSV). The TSV plot is shown in Figure S1 of the supplementary material. The six clusters were defined as shown in Figure 2. This figure shows the frequency of trajectories for each cluster passing through the corresponding grid point and reaching the OPE station at 12:00 UTC. Clusters 1, 2 and 3 are characterised by continental air masses (mostly from south, east and north respectively). Cluster 4 is dominated by slow moving trajectories from the west. Clusters 5 and 6 are dominated by western marine trajectories.

Mis en forme : Normal

2.3 GHG measurements system

The GHG measurements system was setup in 2011 with support from the ICOS Preparatory Phase projects. It was built in order to comply with the Atmospheric Station class 1 stations specifications from ICOS. It relies on a fully automated samples distribution system with remote control backed up by an independent robust spare distribution system. It includes several continuous analysers for the main GHGs (CO_2, CH_4 and N_2O), a manual flask sampler as well asand specific analysers or samplers for tracers such as radon, CO and $^{14}CO_2$.

The continuous GHG measurements system is made of three main parts: an ambient air samples preparation and distribution component, a reference gases distribution component and a master component which is conductsing the main analysis sequence and controlsling the distribution and analysis systems through via pressure and flowrate meters. The stations flow diagram is described inon the Figure 3Figure 3. The aAmbient air is collected at three levels on the tower at the 10m, 50m and 120m levels and brought down to the shelter located at the tower base using 0.5'' inches outer diameter Dekabon tubeings equipped fitted with a stainless steel inlet designed to excludes keep out precipitations. Five sampling lines are installed at 120m,and three are installed at 10m and 50m. From the 120m level, one line is connected to the $14CO_2$ sampler built by the Heidelberg University. Another sampling line is used to collect weekly flask samples. The continuous GHG measurements are done performed using two independent sampling lines. The last line is a spare line which can be operated in case ofof the event of problems trouble on oneanother line or in case offor temporary additional experiments such as independent audits as the oneslike those performed in 2011 or and 2014. At 10m and 50m levels, two lines are used for the continuous GHG measurement system. Another spare line is also installed for each of the 10m and 50m levelBoth of these levels also have a spare line.

At each level, the continuous GHG monitoring system air is flushed from the tower using three Neuberger N815KNE flushing pumps Neuberger N815KNE (15 LPM nominal flow rate) and cleaned by twoa couple of 40 microns and 7 micron s Swagelok stainless steel filters. From each sampling line, a secondary KNF N86KTE-K pump KNF N86KTE-K (5.5 LPM nominal flow rate) is used to sample and pressurisze the air (through a 2 micron Swagelok filter) the air to be dried and then analysed. A flowmeter is used to monitor the air flow in the flushing line and a pressure sensor is used to monitor the sampling line pressure. The air sample is pre-dried by a fridge through in a coil passing through a fridge(to increase the path in the fridge and the residence time). To further dry the sample, the air passes through a 335mL glass trap cooled in an ethanol bath at -50°C using a dewar. Once dried in the cryo water traps (-40°C dew point), the air sample is pressure regulated (~1150 hPa abs at the instrument inlet) and brought directed to the analysers.

The ambient air distribution component is driven by a control control/command component, designed around a Programmable Logic Controller (PLC), which is dedicated to the) for selection and distribution of the ambient air sample from the three sampling heights. This distribution component selects an ambient air sample from one of the three levels using three 3-ways solenoid valves and then root directs it to the drying system and then to the air analysers. Once analysed, the air sample flows

Mis en forme : Exposant

Mis en forme : Indice

back to the distribution panel where a ~~backward~~ back pressure regulator controls the air pressure in the sample line. A pressure sensor monitors the pressure at the analyser inlets and a flow meter monitors the flow rate at the analyser outlets.

~~The control/command component system selects between standards and ambient air, following the PLC's order, the PLC being responsible of the sequence management and quality control processes. The standard gas distribution component is based on a 16 position Vici Valco valve from which nine ports are connected to the analysers. The pressure of the selected standard gas or the ambient air sample is adjusted at the analyser inlet by a manual pressure regulator. All the distributing tubings are stainless steel either 1/8 or 1/4 inches and are over pressurized to avoid any leakage artifact. According to ICOS internal rules, global leakage checks are performed on a yearly basis and after any maintenance operation~~

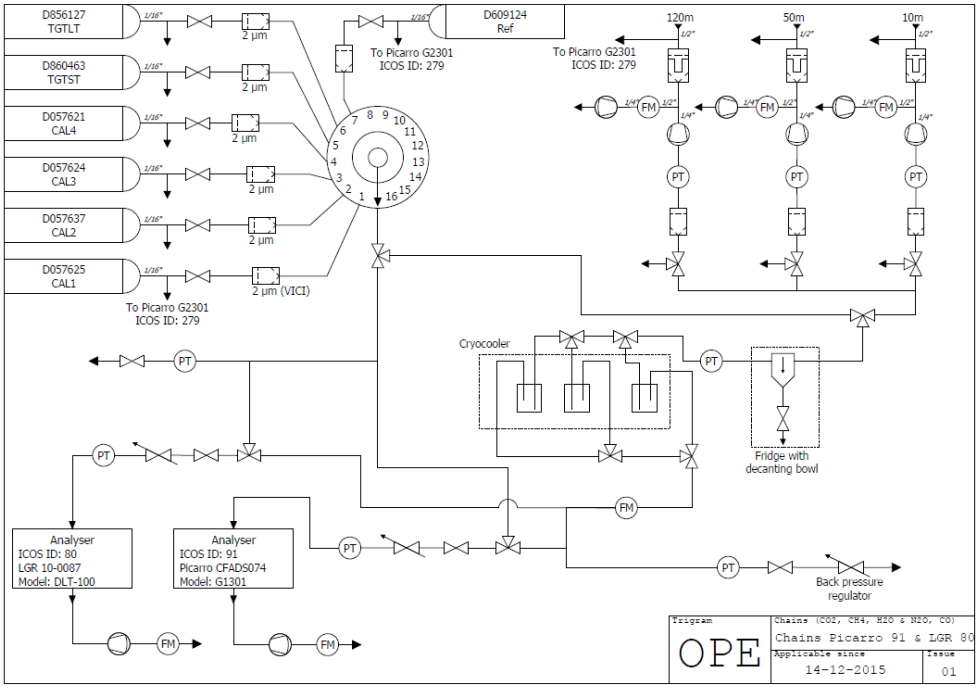

Figure 3: Flow diagram of the OPE GHG measurement system (FM: flow meter, PT: Pressure Transducer)

The control/command component system selects between standards and ambient air, following the PLC's order, as it is responsible for the sequence management and quality control processes. The standard gas distribution component is based on a 16 position Vici Valco valve from which nine ports are connected to the analysers. The pressure of the selected standard gas

or the ambient air sample is adjusted at the analyser inlet by a manual pressure regulator. All the1/8'' or ¼'' stainless steel distributing tubings are over pressurised to avoid any leakage artefact. According to ICOS internal rules, comprehensive leak checks are performed on a yearly basis and after all maintenance operations.

The analysers used are Picarro series G1000 and G2000 cavity ring down spectrometers (CRDS) ~~series G1000 and G2000~~ for CO_2, CH_4, H_2O and CO and Los Gatos Research Off-Axis Integrated Cavity Output Spectroscopy ~~Off-Axis ICOS~~ spectrometers for N_2O and CO. Each analyser used at the station ~~went~~ first underwent ~~through~~ extensive laboratory tests at LSCE during the development of the ICOS Metrology laboratory at ATC (Lebegue et al., 2016, Yver Kwok et al., 2015). These initial tests provide valuable information~~s~~ about the intrinsic properties of the analysers, their precision, stability, water vapour sensitivity and temperature dependence.

Over the ~~period~~ 2011-2018 period, ~~-~~the reference analysers were~~are~~ a Picarro G1301 (ICOS# 91) which performs CO_2 and CH_4 (and H_2O) mole fractions ~~analysis~~analyses and a Los Gatos Research DLT100 (ICOS #80) which is used for CO (and H_2O) mole fraction measurements. A ~~couple of spare and~~redundant pair of parallel instruments have been running either on the ~~principal~~ main distribution system and /or on the spare distribution system ~~following~~ using the same calibration and quality control strategy.

The routine operating sequence includes :~~in a sequence order~~

- Start with a ~~complete~~full calibration ~~of~~including four~~4~~ cycles of ~~4~~four standards lasting 8 hours followed by 30min of Long Term target (LTT) and then by 30min of Short Term target (STT).

~~by 30min of LTT and then by 30min of STT.~~

- 5 hours of ambient air in cycles of three~~3~~ steps of 20min for the 10m level, 50m level and then 120m level
- 20min of Reference gas (REF) ~~REF~~
- 5 hours of ambient air in cycles of ~~3~~three steps of 20min of the 10m level, 50m level and then 120m level
- 20min of STT

During the first years of the ICOS preparatory phase, the calibrations were performed every two weeks. ~~For~~Due to gas consumption issue and ~~after~~following optimization tests, they are now performed ~~on a 3~~every three weeks ~~basis~~.

The routine sequence is summarised in Table S1 in the supplementary materials

The flushing and stabilisation periods for the standards are 10 minutes meaning that the first 10 minutes of data for each of the standards are rejected. The flushing and stabilisation period for the ambient air samples are 5 minutes meaning that the first 5 minutes of data for each of the ambient air levels are rejected (only 15min of~~n~~ the total 20minutes every hour are available).The raw data are then calibrated using the ~~2~~two ~~weeks~~ or ~~3~~three ~~weeks complete~~two or three weekly full calibration and ~~REF~~reference working standards following Hazan et al. (2016). Raw data (between 1s and 5s resolution) are aggregated to one minute~~s~~s and one hour~~ly~~ averages. The results presented here are based on validated minute data from mid 2011 to end of 2018.

The calibrations strategy includes four consecutive cycles of the four calibration cylinders sampled for 30 minutes each, the ~~complete~~ full calibration lasts 8 hours. An archive reference standard gas ~~nicknamed~~ called Long Term Target (LTT) is injected every ~~2~~two or ~~3~~three weeks for ~~a duration of~~ 30 minutes while a common archive reference standard gas ~~nicknamed~~ called Short Term Target (STT) is injected for 20 minutes every 10 hours. Another short term working standard ~~nicknamed~~ called Reference (REF) gas is also used every 10 hours to correct ~~the~~ short term variability. The ~~mole fractions of the standard cylinders concentrations of the standards~~ cover the unpolluted atmospheric range ~~were defined~~ following ~~the ICOs~~ ICOS Atmospheric Station specifications (Laurent, 2017). The standard gases are supplied ~~using~~ via a SCOTT Nickel-plated brass regulator from a 50l Luxfer Aluminium cylinder. Before M~~m~~arch 2016, the standard and performance cylinders used were prepared by LSCE and were traceable to WMO scales (CO_2:WMO X2007, CH_4: WMO X2004A ~~WMOX2007~~, CO: WMO X2014A ~~WMO-CO-X2014~~, N_2O: WMOX2007). Since M~~m~~arch 2016, the standard and performance cylinders used have been prepared by the Central Analytical Laboratories ~~CAL~~ of ICOS (CAL) and are traceable to WMO scales (CO_2:WMO X2007, CH_4: WMO X2004A~~WMO-2004~~, CO: WMO X2014A~~WMO-CO-X2014~~, N_2O: NOAA-2006A ~~NOAA-2006~~). ~~Short Term Target~~STT and ~~Reference~~REF cylinders are refilled every 6 month~~s~~ by ~~the Central Analytical Laboratories of IC~~ICOS-CAL. All the measurement data presented here were recalibrated on these scales.

The raw data from the analysers ~~as well as~~along with the distribution system monitoring parameters are transmitted to the ATC database on a daily basis. Data ~~is~~ are then processed following Hazan et al. (2016) including a specific water vapour correction for the remaining humidity, as well as a station specific automatic flagging process. Data products are then generated ~~allowing a~~so that data quality control ~~regular control of the data quality.~~can be done on a regular basis. Additionally ~~a~~ manual flagging is performed by the station~~'s~~ Principal Investigator (PI) on the raw data ~~as well as~~and on the hourly aggregated data.

Figure 4 gives an overview of the different GHG continuous analysers in operation at the OPE station and their respective time periods. Details on the start and end dates and additional information regarding ancillary instrumentation are in Table S2 in the supplementary material.

Mis en forme : Indice

Mis en forme : Indice

Mis en forme : Indice

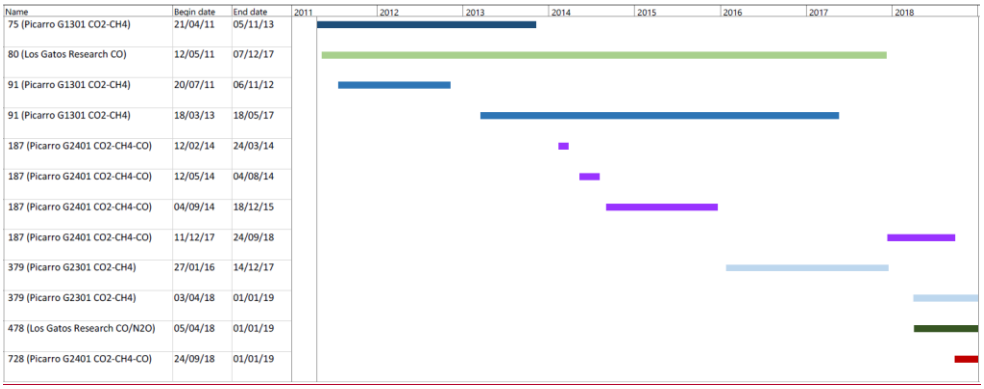

Figure 4: Time diagram showing the different GHG analysers in operation at the OPE station.~~The routine operating sequence includes in a sequence order~~

Mis en forme : Légende

~~- Start with a complete calibration of 4 cycles of 4 standards lasting 8 hours followed by 30min of LTT and then by 30min of STT,~~

Mis en forme : Légende, Sans numérotation ni puces

~~- 5 hours of ambient air in cycles of 3 steps of 20min fo the 10m level, 50m level and then 120m level~~

~~- 20min of REF~~

~~- 5 hours of ambient air in cycles of 3 steps of 20min of the 10m level, 50m level and then 120m level~~

~~- 20min of STT~~

~~During the first years of the ICOS preparatory phase, the calibrations were performed every two weeks. For gas consumption issue and after optimization tests, they are now performed on a 3 weeks basis.~~

Mis en forme : Légende

~~The flushing and stabilisation periods for the standards are 10 minutes meaning that the first 10 minutes of data for each standards are rejected. The flushing and stabilisation period for the ambient air samples are 5 minutes meaning that the first 5 minutes of data for each ambient air levels are rejected (only 15min on the total 20minutes every hour are available). The raw data are then calibrated using the 2 weeks or 3 weeks complete calibration and REF working standards following Hazan et al. (2016). Raw data (between 1s and 5s resolution) are aggregated to minutes and hourly averages. The results presented here are based on validated minute data from mid 2011 to end of 2018.~~

~~For 14CO_2 analyses, two weeks integrated large volume samples of atmospheric CO_2 are also collected from the 120m inlet by quantitative chemical absorption in basic sodium hydroxide (NaOH) solution, as described by Levin et al. (1980). CO_2 samples are then processed in the Heidelberg 14C laboratory by acidification of the NaOH solution in a vacuum system. The extracted CO2 is subsequently purified over charcoal. The 14C/C ratio is then measured by low level counting (Kromer and Münnich, 1992).~~

~~The Table 1 gives an outlook of the different analysers and sensors that were used at the station over different periods.~~

Parameter	Analyser	ICOS Id	Levels	Frequency	Period 1	Period 1	Period 2	Period 2	Period 3	Period 3	Period 4	Period 4
$CO_2/CH_4/H_2O$	Picarro G1301	91	10m / 50m /120m	5s/1min/1h	20/07/2011	06/11/2012	18/03/2013	18/05/2017				
$CO_2/CH_4/H_2O$	Picarro G2301	75	10m / 50m /120m	5s/1min/1h	20/04/2011	07/11/2013						
$CO_2/CH_4/CO/H_2O$	Picarro G2401	187	10m / 50m /120m	5s/1min/1h	12/02/2014	24/03/2014	12/05/2014	03/08/2014	04/09/2014	18/12/2015	11/12/2017	24/09/2018
$CO_2/CH_4/H_2O$	Picarro G2301	379	10m / 50m /120m	5s/1min/1h	27/01/2016	24/11/2017						
$CO_2/CH_4/CO/H_2O$	Picarro G4301	728	10m / 50m /120m	5s/1min/1h	24/09/2018	-						
$CO/N_2O/H_2O$	Los Gatos Research N_2O and CO	80	10m / 50m /120m	1s/1min/1h	13/05/2011	24/11/2017						
$CO/N_2O/H_2O$	Los Gatos Research N_2O and CO	478	10m / 50m /120m	1s/1min/1h	05/04/2018	-						
Wind	Gill Wind Observer		10m / 50m /120m	5s/1min/1h	05/05/2011							
Temperature - Relative Humidity	Vaisala HMP155A		10m / 50m /120m	5s/1min/1h	05/05/2011							
Pressure	RM Young 61302		10m / 50m /120m	5s/1min/1h	05/05/2011							
Radon monitor	U Heidelberg	117	10m	30 min	25/03/2011	22/08/2011						
Radon monitor	U Heidelberg	118	10m	30 min	16/09/2011	05/01/2012						
Radon monitor	ANSTO	546	120m	30 min	10/07/2017							
Integrated NaOH $14CO_2$ sampler	U Heidelberg		120m	2 weeks	25/03/2011	-						
Flask sampler	LSCE		120m	1 week	12/05/2011	15/07/2014	27/05/2015					
Mixing layer height	Lidar Leosphere ALS 300			30s/15min	23/04/2011	15/11/2012	18/01/2013	01/04/2013	30/05/2013	30/07/2013	06/12/2013	03/11/2014

~~**Table 1: Analysers, sensors and samplers, atmospheric parameters, associated ICOS reference number as well as the period of operation at the station**~~

2.4 ~~Composite merged time series~~Data processing

The GHG data cover~~s~~ several years and were collected using different sampling systems and analysers. In each of the individual time series, some data are missing because of either sampling issues, analyser~~'~~s problems or local contamination~~s~~ near the station. Very local pollution~~s due~~, for example due to field works or~~,~~ infrastructure maintenance~~, are very uncommon and~~ occur~~s~~ only rarely. Power outage~~s~~ also ~~happened~~ occurred due to~~because of~~ lighting~~s~~ ~~and~~ or construction work. ~~Troubles~~ Problems on the sampling systems are more frequent and ~~may~~ include tub~~e~~ing leak~~s~~, pump troubles, filter~~s~~ clogging or control/command component system failure. Analyser~~s~~ ~~troubles~~ problems are also quite common and range from software issues, operating system failures, hardware problems (hard disk, fan, etc.~~, …~~), or worse, liquid contamination (from water or ethanol) of the optical cell.

Raw data from the instruments (mole fractions and internal parameters such as cell temperature/pressure, outlet valve), and from the air distribution system (sequence information and ancillary data such as pressure and flow rates in the sampling lines) are transferred at least once a day to the ATC data server. Data are then processed automatically as described in Hazan et al., (2016). Sequence data are used to generate the ambient air and cylinders raw time series. Mole fractions ~~R~~raw data are flagged automatically using the ancillary data based on a ~~ a~~ set of parameters defined for ~~the~~each station and instrument . For the Picarro G1301 #91, G2301 #379 and G2401 # 728 analysers, the internal flagging parameters are the same as the ones shown on Table 4 in Hazan et al. (2016). A manual flag is then applied by the station PI in order to eventually discard data using local station information (e.g. local contamination, maintenance operation, leakage, instrumental malfunctions, etc…). The list of

descriptive flags available to the PI for valid or invalid data is shown in Table 2 of Hazan et al. (2016). Table 1 below presents the quantitative statistical summary of the raw data status for the different instruments used at the OPE station. Details of the internal flagging associated with the flags presented in this table can be found in Table 6 of Hazan et al. (2016). Flag N corresponds to invalid data rejected automatically. Flags O and K correspond to valid and invalid data, respectively, from the manual Quality Control. Between 62 and 72% of the raw data are valid (O) while around 25% of the raw data are automatically rejected (N) , 20% being rejected because of stabilisation/flushing. Corrections related to ~~the~~ water vapour content, and ~~the~~ calibration are then applied. Finally, data are aggregated in time to produce minute, hourly and daily means.

Instrument	Compounds	Start	End	Flag	% raw data
75	CO_2/CH_4	21/04/2011	05/11/2013	O	72.1%
				N	25.80%
				K	2.10%
80	CO	12/05/2011	07/12/2017	O	71.0%
				N	23.5%
				K	5.50%
91	CO_2/CH_4	21/07/2011	22/06/2017	O	67.2%
				N	23.8%
				K	9.00%
187	CO_2/CH_4/CO	12/02/2014	03/04/2018	O	65.1%
				N	30.7%
				K	4.20%
379	CO_2/CH_4	27/01/2016	31/12/2018	O	71.7%
				N	24.9%
				K	3.40%
478	CO	27/01/2016	31/12/2018	O	62.4%
				N	24.9%
				K	12.70%
728	CO_2/CH_4/CO	27/01/2016	31/12/2018	O	65.6%
				N	25.0%
				K	9.40%

Table 1: Flags attributed to raw data from the different instruments between mid 2011 and end of 2018. The last two columns provide the type of flag and the percentage of raw data that were attributed this flag. Flagged O data are valid data manually checked, while N and K flagged are non valid data respectively automatically and manually rejected.

From these individual time series, we built three combined time series for CO_2, CH_4 and CO filling the gaps when possible The objective is to provide users with continuous time series, combining valid measurements in order to minimise the data gaps. Before merging the time series, each instrument is quality controlled individually, and only measurements which are validated by the automatic data processing and the PI are considered for the combined dataset. For each measurement we indicate the reference of the measuring instrument (unique identifier in the ICOS database), providing the user with analyser traceability. To build these times series from various analyser datasets we used the priority order given in Table 2 for CO_2 and CH_4 and Table 3 for CO. The priority order is defined a priori by the station PI considering which analysers are fully dedicated to the station for long term monitoring purposes. In general secondary instruments are installed for shorter periods to perform specific additional experiments (like dry vs humid air samples, line tests, flushing flow rate tests, etc). For example, 91 was the main instrument for CO_2 and CH_4 followed by 379. While 91 was in maintenance, instruments 75 or 187 were used as spare instruments. At the beginning of 379 operation, 91 was still the main instrument, to maintain time series consistency as

Mis en forme : Centré

Mis en forme : Légende

Mis en forme : Indice

Mis en forme : Indice

Mis en forme : Indice

Mis en forme : Indice

Mis en forme : Indice

Mis en forme : Indice

long as possible. When 91 operation stopped, 379 became the main instrument. When 379 was in repair, instrument 187 was used as a spare instrument again. For CO, the LGR analyser 80 was the main instrument followed by Picarro G2401 728. When the LGR 80 was out of order, we used either Picarro 187 or LGR 478 as spare instruments. When two instruments are installed for long-term measurements, the priority order should take into consideration the performance of each one. It is the responsibility of the station manager to change the priority list in the ICOS database if needed. ~~From these individual time series, we built three combined time series for CO_2, CH_4 and CO filling the gaps when possible using only « real » observations (but not using any synthetic data from models). To build these times series from the different analyser's dataset we use the priority order given in Table 2.~~Merging the individual time series in such a way implies that the merged time series show steps in their uncertainties as individual analysers have different performance (see Part 3 Data Quality Assesment for details about the steps in repeatability performance).

Mis en forme : Justifié

Compound	Main analyzer	Spare analyzer	Start Date	End Date
CO_2 / CH_4		75 (Picarro G1301)	21/04/2011 00:00	20/07/2011 23:00
CO_2 / CH_4	91 (Picarro G1301)	75 (Picarro G1301)	21/07/2011 00:00	05/11/2013 23:00
CO_2 / CH_4	91 (Picarro G1301)	-	06/11/2013 00:00	11/02/2014 23:00
CO_2 / CH_4	91 (Picarro G1301)	187 (Picarro G2401)	12/02/2014 00:00	27/01/2016 00:00
CO_2 / CH_4	91 (Picarro G1301)	379 (Picarro G2301)	27/01/2016 00:00	22/06/2017 00:00
CO_2 / CH_4	379 (Picarro G2301)	-	22/06/2017 00:00	14/12/2017 00:00
CO_2 / CH_4		187 (Picarro G2401)	14/12/2017 00:00	03/04/2018 14:00
CO_2 / CH_4	379 (Picarro G2301)	-	03/04/2018 14:00	24/09/2018 14:30
CO_2 / CH_4	379 (Picarro G2301)	728 (Picarro G2401)	24/09/2018 14:30	-

Compound	Instrument 1	Instrument 2	Start Date	End Date
CO_2	75 (Picarro G1301)	-	21/04/2011 00:00	20/07/2011 23:00
CH_4	75 (Picarro G1301)	-	21/04/2011 00:00	20/07/2011 23:00
CO	80 (Los Gatos CO/N_2O)	-	12/05/2011 00:00	07/11/2012 00:00
CO_2	91 (Picarro G1301)	75 (Picarro G1301)	21/07/2011 00:00	05/11/2013 23:00
CH_4	91 (Picarro G1301)	75 (Picarro G1301)	21/07/2011 00:00	05/11/2013 23:00
CO	80 (Los Gatos CO/N_2O)	-	11/03/2013 00:00	12/02/2014 00:00
CO_2	91 (Picarro G1301)	-	06/11/2013 00:00	11/02/2014 23:00
CH_4	91 (Picarro G1301)	-	06/11/2013 00:00	11/02/2014 23:00
CO	187 (Picarro G2401)	80 (Los Gatos CO/N_2O)	12/02/2014 00:00	18/12/2015 00:00
CO_2	91 (Picarro G1301)	187 (Picarro G2401)	12/02/2014 00:00	27/01/2016 00:00
CH_4	91 (Picarro G1301)	187 (Picarro G2401)	12/02/2014 00:00	27/01/2016 00:00
CO	80 (Los Gatos CO/N_2O)	-	18/12/2015 00:00	07/12/2017 00:00
CO_2	91 (Picarro G1301)	379 (Picarro G2301)	27/01/2016 00:00	22/06/2017 00:00
CH_4	91 (Picarro G1301)	379 (Picarro G2301)	27/01/2016 00:00	22/06/2017 00:00
CO_2	379 (Picarro G2301)	-	22/06/2017 00:00	14/12/2017 00:00
CH_4	379 (Picarro G2301)	-	22/06/2017 00:00	14/12/2017 00:00
CO_2	187 (Picarro G2401)	-	14/12/2017 00:00	03/04/2018 14:00
CH_4	187 (Picarro G2401)	-	14/12/2017 00:00	03/04/2018 14:00
CO	187 (Picarro G2401)	-	14/12/2017 00:00	05/04/2018 18:00
CO_2	379 (Picarro G2301)	187 (Picarro G2401)	03/04/2018 14:00	24/09/2018 14:00
CH_4	379 (Picarro G2301)	187 (Picarro G2401)	03/04/2018 14:00	24/09/2018 14:00
CO	187 (Picarro G2401)	478 (Los Gatos CO/N_2O)	05/04/2018 18:00	10/09/2018 14:00
CO	187 (Picarro G2401)	478 (Los Gatos CO/N_2O)	10/09/2018 14:00	24/09/2018 14:00
CO	478 (Los Gatos CO/N_2O)	-	24/09/2018 14:00	24/09/2018 14:30
CO_2	379 (Picarro G2301)	-	24/09/2018 14:00	24/09/2018 14:30
CH_4	379 (Picarro G2301)	-	24/09/2018 14:00	24/09/2018 14:30
CO	728 (Picarro G2401)	478 (Los Gatos CO/N_2O)	24/09/2018 14:30	17/01/2019 09:59
CO_2	379 (Picarro G2301)	728 (Picarro G2401)	24/09/2018 14:30	17/01/2019 09:59
CH_4	379 (Picarro G2301)	728 (Picarro G2401)	24/09/2018 14:30	17/01/2019 09:59

Table 22: Order of priority (main vs spare analysers) for the CO_2 and /CH_4/CO compounds with ICOS instrument identifiers and associated period

Various instruments were used in parallel for some time and it is thus possible to assess systematic differences between the data for these common periods. The instruments may have shared sampling tubes, calibration and quality control gases but may have also used different air distribution system and different cylinders. Consequently, differences may occur due to problems associated with time synchronisation, air sampling (sampling and flushing pump efficiencies), calibration and water correction or other causes not yet identified.

Compound	Main analyzer	Spare analyzer	Start Date	End Date
CO	80 (Los Gatos CO/N_2O)	-	12/05/2011 00:00	07/11/2012 00:00
CO	80 (Los Gatos CO/N_2O)	-	11/03/2013 00:00	12/02/2014 00:00
CO	80 (Los Gatos CO/N_2O)	187 (Picarro G2401)	12/02/2014 00:00	18/12/2015 00:00
CO	80 (Los Gatos CO/N_2O)	-	18/12/2015 00:00	07/12/2017 00:00
CO		187 (Picarro G2401)	14/12/2017 00:00	05/04/2018 18:00
CO	187 (Picarro G2401)	478 (Los Gatos CO/N_2O)	05/04/2018 18:00	24/09/2018 14:00
CO		478 (Los Gatos CO/N_2O)	24/09/2018 14:00	24/09/2018 14:30
CO	728 (Picarro G2401)	478 (Los Gatos CO/N_2O)	24/09/2018 14:30	-

Table 3: Order of priority (main vs spare analysers) for CO with ICOS instrument identifiers and associated period

The different instruments were used in parallel for some time and it is thus possible to assess the systematic differences between the data for these common periods. The instruments may have shared sampling tubes, calibration and quality control gases but may have also used different air distribution system and different cylinders. Consequently, differences may occur due to troubles in time synchronisation, air sampling (sampling and flushing pumps efficiency) , calibration and correction or any other causes not yet identified.

The Figure 5Figure 4 shows the mean afternoon (12:00-17:00 UTC) hourly data difference between the different instruments analysing ambient air at the 120m level for CO_2 and CH_4. Large deviations in the afternoon means are revealed by such comparison. Summary statistics for the differences shown in Figure 5 for the 120m level (and for the 10m and 50m levels) are given in Table S3 of the supplementary materials. On average, over the full period, the differences at 120m are -0.002 ppm for CO_2 and -0.27 ppb for CH_4, below the GAW/WMO compatibility goals (0.1ppm for CO_2 and 2ppb for CH_4). These large significant deviations may come from various uncertainty sources of uncertainty, such as differing residence time difference in the sampling systems, water vapour correction, clock issues, or internal analyser uncertainties.

Mis en forme : Centré

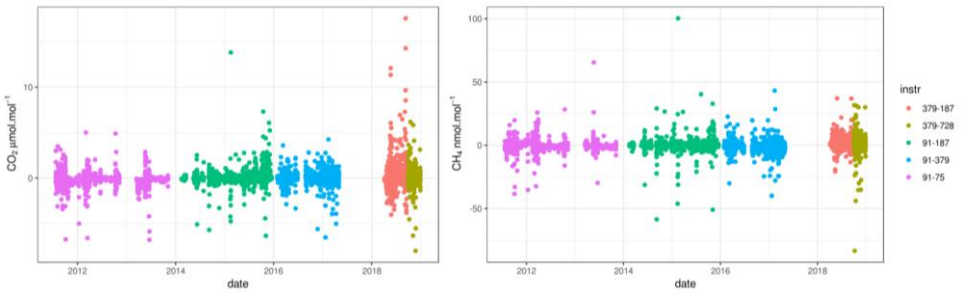

Figure 54: Difference between hourly mean afternoon (12:00-17:00 UTC) data at the top level 120m from the two instruments used at the same time at the OPE station from 2011 to 2018 for CO_2 (left panel) and CH_4 (right panel). The different instruments couples pairs are shown in colour and their identifiers are labelled in the legend key of by the right panel.

Mis en forme : Indice

Mis en forme : Indice

No data filtering was applied regarding the differences and the overall biases are small (Table S3). Large differences can be observed over short periods, especially when the atmospheric signal shows very high variability. For such atmospheric conditions any difference in the time lag between air sampling and measurement in the analyser cell has a significant influence. The persistent presence of a bias between two instruments is used as an indication to perform checks on instruments and air intake chains. For large differences, one of the instruments is generally disqualified based on the tests performed. In the case of moderate differences, the objective is to use this information for estimating uncertainties.

In a similar approach, Schibig et al. (2015) have shown reported results of from the comparison between CO_2 measurements from two continuous analysers run in parallel at the Jungfraujoch GAWJFJ station in Switzerland. The hourly means of the two analysers showed a general good agreement, with mean differences ofn the order of 0.04 ppm (with a standard deviation of 0.40ppm). However large significant deviations of several ppm were also found.

2.5 Data processing

Raw data from the instruments (mole fractions and internal parameters such as cell temperature/pressure, outlet valve), and from the air distribution system (sequence information and ancillary data such as pressure and flow rates in the sampling lines) are transferred at least once a day to the ATC data server. Data are then processed automatically as described in Hazan et al., (2016). Raw data are flagged using a set of parameters defined for the station and instrument. A manual flag is then applied by the station PI in order to eventually discard data using local station information (e.g. local contamination, maintenance operation, leakage, instrumental malfunctions, etc…). Corrections related to the water vapour content, and the calibration are then applied. Finally, data are aggregated in time to produce minute, hourly and daily means.

The hourly time series exhibit strong variability from hourly to decennial time scale. These variations may be related to meteorological and climate changes, and to sources and sinks variations. We are mostly interested in the regional signatures at scales that can be approached by the model inversion and assimilation framework. For this reason we want to isolate from

~~the time series and data aggregation the situations where the local influence is dominant and is shadowing the regional signature. We then need to define the background signal on top of which the regional scale signal is added.~~

~~Such local situations and background definitions may be extracted purely from time series analysis procedures, or may be constrained on a physical basis. The main difficulty is to correctly define the baseline signal of the measured time-series and to adequately flag local spikes. El Yazidi et al. (2018) have assessed the efficiency and robustness of three statistical spikes detection methods for CO_2 and CH_4 and have concluded that the two automatic SD and REBS methods could be used after a proper parameters specification. We used the El Yazidi et al. (2018) method on the composite merged minute time series to filter out « spike » situations. From this despiked minute dataset we built hourly means, which were used to analyse the diurnal cycles. Focusing on data with regional footprints, we selected only afternoon data with low hourly variability (estimated from minute standard deviations). We applied the CCGCRV curve fitting program from NOAA (Thoning et al., 1989) to determine the trend and the detrended seasonal cycle of the afternoon means time series for all species. Residuals from the trends and seasonal cycles were then computed.~~

3. Data Quality Assessment

QA/QC protocols are applied at several steps ~~of~~ in the measurement~~s~~ system. ~~On a daily basis~~Every day, a conservative quality control is ~~operated~~ conducted from two complementary ~~sides~~standpoints: ~~On one side~~firstly, ~~the spectrometers~~ intrinsic properties of the spectrometers are ~~verified~~ ,verified, and ~~the other one side~~secondly, the sampling system parameters are checked. On a weekly to monthly basis, the field performance of the spectrometers ~~performances are~~is also ~~monitored~~checked. A flask program also runs in parallel and is used to expand the atmospheric monitoring to other trace gases and ~~but also~~ to assess the quality of the continuous measurements. Up to now, flask~~s~~ data were not fully available or were contaminated, and thus ~~were not~~have not been used in the present work. A complementary approach to assess compatibility ~~employs~~ uses round robin or ~~so-called~~ "cucumbers" cylinders circulated between stations within the ICOS European network. ~~Finally~~Finally, the station compatibility is also assessed during in situ audits using a mobile station and travelling instruments (Hammer et al, 2013, Zellweger et al., 2016).

In this section we used two metrics defined in Yver Kwok et al. (2015) for ~~the~~ quality control assessment of the data. These two metrics are usually calculated under measurement repeatability ~~conditions of measurements where~~conditions where all conditions stay identical over a short ~~period of time~~period. ~~The c~~Continuous measurement repeatability (CMR), sometimes called precision, is a repeatability measure applied to continuous measurements. ~~The l~~Long-term repeatability (LTR), sometimes called reproducibility, is a repeatability measure over an extended period of time. As ICOS targets the WMO/GAW compatibility goals within its atmospheric network, the analysers must comply with the performance requirements specified in Table 3 of the ICOS Atmospheric Station specifications report (Laurent 2017). ICOS precision limits for CO_2, CH_4 and CO measurements are 50 ppb, 1 ppb and 2ppb respectively. ICOS reproducibility limits for CO_2, CH_4 and CO measurements are 50 ppb, 0.5 ppb and 1ppb respectively.

Mis en forme : Indice

Mis en forme : Indice

3.1Short term target quality control: Field continuous measurement repeatability equivalent

In our basic measurements sequence, the air from a high-pressure cylinder (STT) is analysed twice a day with a 10 ten hours frequency for at least 20 minutes to assess the daily performance of the spectrometers. This metric mainly describes the intrinsic performance of the spectrometers and not of the sampling system. It is a field estimation of the CMR and is computed as the standard deviations of the raw data over 1 min intervals, the first 10 minutes of each target gas injection being filtered out as stabilisation.

The Figure 6Figure 5 shows the monthly means CMR of for the combined time series of CO_2 and CH_4 using the same type of analysers. The time series of CO's CMR- for CO o are not shown in the supplementary materials (Figure S2).as the intrinsic properties of the Picarro and Los Gatos Research analysers are very different making it difficult to compare on a same plot. For CO_2, we observe a decrease of the CMR over the measurement periods, indicating an improvement of in the instruments precision. The Analyserspectrometer #91 (CRDSPicarro, G1301) was shipped to the manufacturer for a major repair including cell replacement between November 2012 and March 2013. The repair at the Picarro workshop improved the CMR performance of the analyser from above more than 0.06 to below less than 0.05 ppm. For this instrument, the factory estimated a CMR of 0.04 ppm in 2009 and the lab test at ATC metrology laboratory (-MLab) in 2012 estimated a CMR of 0.06 ppm.

Figure 65: Monthly mean field Continuous Measurement Repeatability (CMR) for CO_2 (left panel), and CH_4 (right panel) estimated over time for the different instruments in operation at the OPE station over the 2011-2018 period. The different instruments are shown in colorcolour and and their identifiers are labelled in the legend of the top and bottomkey by the right panels. Some months, have several instruments running at the station and these are identified with several labels.s

Using a gas chromatograph at the Trainou (TRN) tall tower, Schmidt et al. (2014) found a mean standard deviation of in the hourly target gas injections of 0.14 ppm for CO_2, 3.2 ppb for CH_4 and 1.9 ppb for CO for the whole period of 2006-2013. Berhanu et al. (2016) presented their system performance using precision, a metric based on the standard deviation of the 1-min target gas measurements, at 0.05ppm for CO_2, 0.29ppb for CH_4 and 2.79ppb for CO using a Picarro G24010 spectrometer over 19 months from 2013 to 2014. Lopez et al. (2015) presented STR short term repeatability (a metric similar to CMR)

estimates for the gas chromatograph system used at Puy de ~~dôme~~ Dôme (PDD) at 0.1ppm for CO_2 and 1.2 ppb for CH_4, for the years 2010-2013. Table S4 of the supplementary materials summarises this information.

~~The~~ Table 4~~Table 3~~ presents the comparison of the CO_2 and CH_4 CMR for the instruments #75/91/187/379/728 estimated by the manufacturer~~,~~ and by the ICOS ATC MLab ~~as well as~~along with the mean values from ~~the~~ station measurements over the 2011-2018 period. The station performance of each individual analyser is ~~coherent~~ consistent with its performance estimated at the factory and at the ATC MLab. ~~The p~~Performances ~~are~~is maintained over several years and ~~were~~ was not disturbed by the station setting~~s~~.

		CO_2 (ppm)			CH_4 (ppb)		
Analyser	ICOS Id	factory CMR	ATC Mlab CMR	Field mean CMR	factory CMR	ATC Mlab CMR	Field mean CMR
Picarro G1301	91	0.04	0.059	0.048	0.27	0.24	0.27
Picarro G1301	75	0.019	0.022	0.02	0.18	0.26	0.22
Picarro G2401	187	0.023	0.026	0.021	0.2	0.28	0,22
Picarro G2301	379	0.025	0.023	0.022	0.23	0.22	0.2
Picarro G2401	728	0.014	0.013	0.014	0.1	0.09	0.08

		CO_2 (ppm)			CH_4 (ppb)		
Analyser	ICOS Id	factory CMR	ATC Mlab CMR	Field mean CMR	factory CMR	ATC Mlab CMR	Field mean CMR
Picarro G1301	91	0.04	0.059	0.048	0.27	0.24	0.27
Picarro G1301	75	0.019	0.022	0.02	0.18	0.26	0.22
Picarro G2401	187	0.023	0.026	0.021	0.2	0.28	0.22
Picarro G2301	379	0.025	0.023	0.022	0.23	0.22	0.2
Picarro G2401	728	0.014	0.013	0.014	0.1	0.09	0.08

Table ~~4~~3: Continuous measurement repeatability (CMR) estimated by the factory, MLab and field means over 2011-2018 ~~of~~ for CO_2 (ppm) and CH_4 (ppb). ~~Their~~ Instrument model and ICOS Identifier are indicated in the first columns.

For CH_4, the factory estimated CMR~~'s~~ for instrument #91 in 2009 was 0.27ppb and the initial lab tests at ATC MLab in 2012 estimated CMR for CH_4 at 0.24 ppb. The repair at the Picarro workshop did not modify the CMR performance of the analyser. For each instrument, the CH_4 performance ~~are~~ is very stable ~~along~~ over the years with very few outliers.

The CO performance~~s~~ (CMR and LTR) estimated at the station ~~are~~ is compared to the factory and ATC MLab results in ~~the~~ Table 5~~Table 4~~.

		CO (ppb)				
Analyser	ICOS Id	factory CMR	ATC Mlab CMR	Field mean CMR	ATC Mlab LTR	Field mean LTR
Los Gatos N_2O and CO	80	0.15	0.06	0.06	0.3	0.4
Picarro G2401	187	6.5	5.7	5.17	1.7	1.18
Los Gatos	478	0.06	0.09	0.05	0.09	0.05
Picarro G2401	728	2.7	2.69	2.76	0.22	0.33

		CO (ppb				
Analyser	ICOS Id	factory CMR	ATC Mlab CMR	Field mean CMR	ATC Mlab LTR	Field mean LTR
Los Gatos N_2O and CO	80	0.15	0.06	0.06	0.3	0.4
Picarro G2401	187	6.5	5.7	5.17	1.7	1.18
Los Gatos	478	0.06	0.09	0.05	0.09	0.05
Picarro G2401	728	2.7	2.69	2.76	0.22	0.33

Table 54: Continuous measurement repeatability (CMR) and long-term repeatability (LTR)) between factory, MLab and field mean over 2011-2018 of CO (ppb). Their model and ICOS Identifier are indicated in the first columns.

Mis en forme : Centré

The ~~CO~~ CMR time series for CO (~~not shown~~Figure S2 of the supplementary materials) displays four different periods which are directly linked to the analysers used to build the ~~combined~~ merged time-series. We used two different types of analyser~~s type~~: one ~~build~~ built by Los Gatos Research ~~based on the ICOS technology~~ (instruments #80 and #478) and one built~~d~~ by Picarro ~~based on the CRDS technology~~ (instruments #187 and #728). These two types of analyser~~s~~ have very different internal properties as can be seen in Table 5. ~~The CO CMR results reflect such large differences making it difficult to show direct comparison~~ (shown in Figure S2 of the supplementary materials), the CO CMRs from Los Gatos Research instruments being much lower than the CO CMRs from Picarro. The Picarro 187 and 728 CO LTRs are significantly lower than their CO CMRs. This means that their raw data have large high ~~-~~frequency variabilities but when averaged over several minutes these instruments are quite stable (they are not very sensitive to atmospheric or pressure changes).

Overall the precisions measured at the station for CO_2, CH_4 and CO remain ~~comparable~~ similar to the initial values estimated by the manufacturer and the ATC laboratory, showing no degradation due to the design of the station or the measurement procedures.

3.2 ~~Short term target quality control:~~ Field long term repeatability

The field LTR is computed as the standard deviation of the averaged STT measurement intervals over 3 days as it is done during the initial test at the ICOS Metrology Lab. Data are then averaged every month. The same STT data ~~as previously~~ are used but with a different perspective, more closely linked to the ambient air data uncertainty.

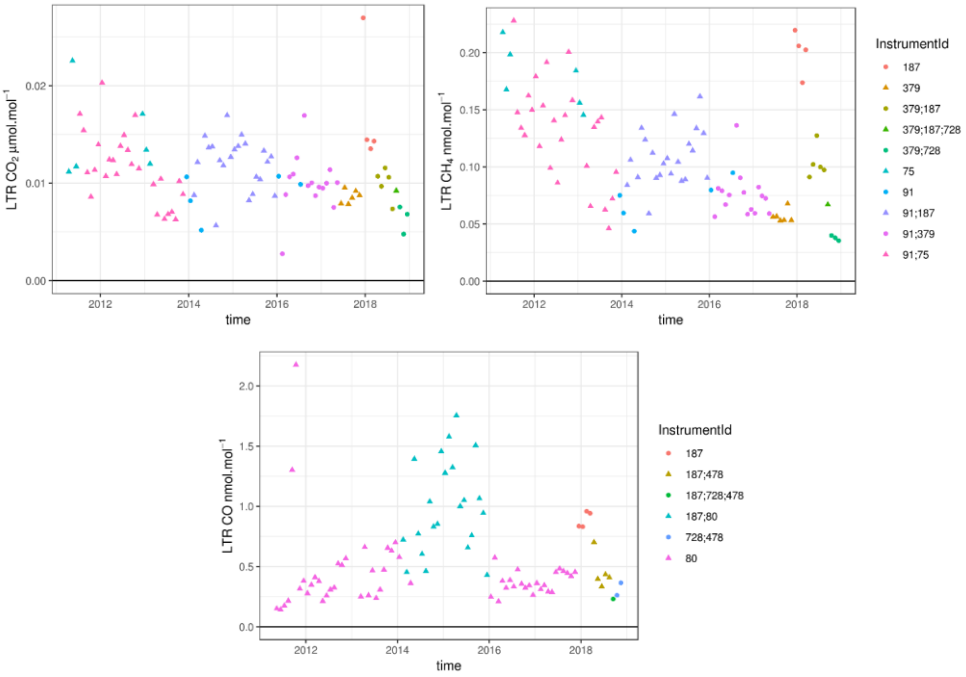

Figure 76: Monthly mean field long term repeatability (LTR) for CO_2 (top left panel), CH_4 (top right panel) and CO (bottom panel) estimated over time for the different instruments in operation at the OPE station over the 2011-2018 period. The different instruments are shown in ~~colour~~colour and their identifiers are labelled in the ~~legend~~ keys of the top and bottom panels. Some months~~,~~ have several instruments running at the station and these are identified with several labels.

~~The~~ Figure 7~~Figure 6~~ shows the monthly mean field LTR of the merged time series using the different instruments and sampling systems. This figure shows the uncertainties of the data related to the analysers (not the sampling systems). As for CMR, CO_2 and CH_4 LTR show decreasing trends suggesting an improvement of the internal performance of the spectrometers built by Picarro, of the air distribution system ~~as well as~~and data selection/flagging. The ~~beginning~~ early part of 2018 experienced a ~~clearly~~ markedly worse~~t~~ LTR compared to neighbouring months. This is mostly due to the use of ~~the~~ instrument #187, which ha~~vs~~e relatively poor performance compared to other instruments.

		CO_2 (ppm)		CH_4 (ppb)	
Analyser	ICOS Id	ATC Mlab LTR	Field mean LTR	ATC Mlab LTR	Field mean LTR
Picarro G1301	91	0.02	0.01	0.08	0.08
Picarro G1301	75	0.01	0.01	0.21	0.17
Picarro G2401	187	0.02	0.02	0.22	0.17
Picarro G2301	379	0.007	0.009	0.1	0.06
Picarro G2401	728	0.005	0.008	0.06	0.02

Table ~~6~~5: Long term repeatability (LTR) of CO_2 (ppm) and CH_4 (ppb) estimated by MLab and field mean over 2011-2018 ~~of CO_2 (ppm) and CH_4 (ppb). Their~~ Instrument model and ICOS Identifier are indicated in the first columns.

The comparison of the field mean LTR and ATC MLab LTR for the different instruments are shown in ~~on the~~ Table 6~~Table 5~~ for CO_2 and CH_4. The LTR field performance of the analysers are ~~in agreement~~consistent with their initial assessments. Periods of lower CO_2/CH_4 LTR are associated with instruments #91, #379 or #728 while periods with ~~larger~~ higher CO_2/ CH_4 LTR are associated with instruments #75 or #187.

As for CMR, the CO LTR monthly time series shows four different periods but with a smaller contrast, ~~related~~ associated with the type of analyser~~s type~~ used at the station. Most periods with LGR instruments (#80 or #478) show~~s~~ a LTR under 0.7 ppb while periods with Picarro instrument #187 show as ~~as~~ LTR above 0.5 ppb.

Different periods have different uncertainty levels related to ~~the~~ instrument performance. While Los Gatos Research instruments show lower CO LTR~~s~~ they have stronger temperature sensitivities generating ~~strong~~ high short-term variability in conditions where the temperature is not well ~~constrained~~controlled. Corrections for these temperature induced biases ~~implied~~ required the frequent use of a working standard~~. quite frequently~~

3.3 Station audit by travelling instruments

A metric such as CMR is very useful ~~to~~ for monitoring the ~~instrument~~ internal performance of instruments and ~~therefore to be~~for ~~able to~~ identifying any instrument failure as ~~soon~~early as possible ~~any instrumental failure~~. Other instrument related metrics such as calibration long term drift or calibration stability over the sequences are also useful ~~to~~ for monitoring ~~the~~ instrument performance. However, they do not give an assessment of the overall measurement systems. Flask versus in-situ comparisons, or station audit by travelling instruments are recogni~~z~~sed as essential tools in the performance and compatibility assessment of a measurement system. ~~The~~ ICOS audits are performed by a mobile lab, hosted by the Finnish Meteorological Institute in Helsinki, and equipped with state of the art GHG analysers and travelling cylinders. The measurements data from the station are centrally processed at the ATC. However, ~~but~~ the data produced by the Mobile Lab~~, however,~~ are ~~calculated~~ computed separately to maintain the independent nature of the Mobile Lab and at the same time to evaluate the performance of the centralised data processing.

The OPE station was audited ~~two times~~twice, once in summer 2011, soon after the station was set up, during the feasibility study ~~of~~ for the travelling instrument methodology and then in summer 2014, when the ICOS Mobile Lab was ready for

operation. During the two week~~s~~ intercomparison in 2011, significant differences for CO_2 and CH_4 were noticed between the Fourier Transform Infrared (FTIR) ~~FTIR~~ travel~~l~~ling instrument and the CRDS reference instrument (Hammer et al., 2013). As the two instruments have different temporal resolutions and different response times, the CRDS measurements were convoluted with an exponential smoothing kernel representing a 3 min turn-over time to match the FTIR specifications. For CO_2 the smoothed differences vary between 0.1 and 0.2 ppm with a median difference of 0.13 ppm and a scatter of the individual differences ~~on the order~~ of approximately ~~±~~0.15 ppm. The smoothed CH_4 differences decrease from ~~initially~~ 0.7 ppb initially to 0.1 ppb, the median difference being 0.4 ppb. Such large differences were caused by relatively poor performance~~s~~ of the CRDS and FTIR instruments because of specific hardware problems ~~but also related~~and also due to ~~to~~ the large temperature variations (10 K) within the measurement~~s~~ container. During the ~~same 2011~~ summer of 2011, the travelling instrument was also set up at the Cabauw (CBW) station in the Netherlands. The audit showed better instrument performance but the same kind of differences for ambient air comparisons. While the CO_2 deviations at CBW were partly explained by a travelling instrument intake line drawback and by calibration issues on the main measurement~~s~~ system, at OPE no final explanation has been found for the observed differences ~~have been found~~.

~~During~~ In the summer of 2014, the two months audit was performed using a Picarro G2401 travelling instrument ~~as well as~~and a FTIR. ~~Nevertheless~~ However the FTIR performance was not yet optimi~~z~~sed and the difference ~~of~~ in time resolution made it difficult to use it properly. Results from this instrument are not considered here. On average, t~~T~~he OPE standard cylinders analysed by the travelling instrument showed ~~on average~~ 0.03 ppm and 0.10 ppm higher CO_2 mole fractions ~~concentrations in~~at the beginning and ~~in~~ at the end of the audit, respectively, than the assigned values used to calibrate measurements at OPE. Similar results were found for CH_4 with relatively low differences ranging between 0 and 1 ppb. The instruments ~~as well as~~and the working standards (OPE and travelling standards) were calibrated against two different sets of standards ~~sets~~, introducing biases in the measurements of cylinders ~~but also~~and of ambient air. The intercomparison was complicated by the fact that the station was ~~hit~~ struck by ~~three~~ lightning~~s~~ three times during the summer, ~~creating~~ causing major power outage~~s~~ and electrical damage~~s~~ to the infrastructure~~s~~. Such power outages generate shifts in the CRDS analyser response that prevent drift correction of the calibration response, degrading ~~the~~ analyser performance. The ambient air comparison was based on two sampling lines, one line ~~supplying~~ delivering ~~a dried~~dry air samples to Picarro G1301 ~~(~~ #91~~)~~ and wet air samples to ~~a wet~~ Picarro G2401 ~~(~~#187~~)~~, and one independent line for the audit supplying wet air samples to the ~~wet~~ travelling instrument (TI). The wet air measurement data from analyser #187 ~~OPE G2401~~ data were corrected for water vapour by the factory Picarro correction, but the ~~travelling instrument~~TI wet air measurement data were~~as~~ corrected by an improved water correction based on water droplet test performed at the beginning of the intercomparison ~~and~~ using a simplified version of the Method #2-EMPA implementation presented in Rella et al. (2013). The ambient air ~~mole fractions for~~ CO_2 mole fractions measured in dry and wet air samples by ~~both dried and wet~~the OPE analysers showed lower mole fractions ~~concentrations~~ compared to the ~~wet travelling instrument~~TI measurements, by 0.10 ppm at the beginning of the audit, and 0.13 ppm at the end. Most of the differences in ambient air measurements can be explained by the bias in the reference scales.

When averaged over the whole period the OPE minus ~~travelling instrument~~TI measurements differences remain within the WMO/GAW ~~component~~ compatibility goal. The OPE ~~dried~~ Picarro G1301 #91 dry air measurements deviated on average by -0.05 ppm compared to the travelling ~~wet~~ Picarro G2401 ~~travelling instrument~~wet air measurements in the case of CO_2, and by 0.70 ppb in the case of CH_4. Similarly the OPE ~~wet~~ Picarro G2401 #187 wet air measurements differ~~s~~ from the travelling instrument wet air measurements by -0.03 ppm and 1.80 ppb for CO_2 and CH_4, respectively. The CO comparison ~~of CO was~~ was carried out ~~made~~ for OPE-LGR and OPE-G2401 instruments and compared to the ~~travelling instrument~~TI G2401: the average deviations ~~were either larger than or barely within~~exceeded the WMO/GAW component compatibility goal (±2 ppb). Vardag et al. (2014) presented similar intercomparison results at MHD ~~Mace Head during~~ over two months in spring 2013. For CO_2, the difference ~~in ambient air measurements at Mace Head~~ between the ~~travelling instrument~~TI and the station analyser (Picarro G1301) for ambient air measurements at MHD ~~was~~ was 0.14±0.04ppm. During this intercomparison there ~~was~~ were no ~~scale~~ calibration issue~~s~~ as the same ~~scale~~ set of calibration cylinders was used on both system~~s~~. However ~~but~~ there could also have been ~~also~~ a bias in the water correction effect. Still, most of the differences between ~~the~~ station data and the TI ~~travelling instrument~~ during ~~,~~ ambient air measurements remained unexplained. The~~se~~ ~~present~~ results ~~as well as~~and the previously published results highlight the major difficulties that station PI~~²~~s are facing with ~~the~~ intercomparison interpretation and understanding. Upcoming sampling line test~~s~~, which are mandatory in the ICOS network at least on a yearly basis, may help ~~to~~ us understand if the sampling design introduces artefacts.

3.4 Travelling "C~~c~~ucumbers" cylinders and station target tank biases

At the beginning of ~~the~~ station operation, quality control tanks, or targets, were not systematically used or ~~, neither~~ calibrated. ~~C~~Calibrated tanks were used systematically from 2015 as working standards ~~allowing~~ in order to monitor biases ~~monitoring~~.

In addition the OPE station took part in the CarboEurope « Cucumber » program in the EURO2 loop at the end of 2014, as well as in the ICOS program which started in September 2017. The aim of these programs is to assess measurement compatibility and to quantify potential offsets in calibration scales within a network. The results of these two sequences of « Cucumbers » intercomparison are shown in Figure 8 along with the biases estimated for the station quality control cylinders.

The biases estimated from the target tanks operated at the station and the blind Cucumber intercomparison biases are consistent for all species. CO_2 biases are found to be between -0.1ppm and 0.1ppm most of the times except for some outliers that still need to be understood. A slight trend may be present in the LTT CO_2 biases between 2014 and 2018. The STT results may show a trend as well but step changes are also present. We attribute the CO_2 biases signal to the convolution of step changes and an interannual trend. The step changes may be due to cylinder changes. The possible CO_2 trend shown by the LTT (of the order of +0.02 ppm) remains unexplained at this stage. The re-evaluation of the CO_2 mole fractions of calibration tanks at the ICOS central facility could show a drift in their values, which would lead to a correction of the time series.

CH_4 biases are between -0.75ppb and 0.75ppb for most cases. CO biases show a large spread at the beginning of station operation partly related to the temperature sensitivity of the Los Gatos Research analyser and the poor temperature control of the measurements container. Since 2016 the CO biases stay within the -5 ppb/+5 ppb range.

Mis en forme : Indice

Mis en forme : Indice

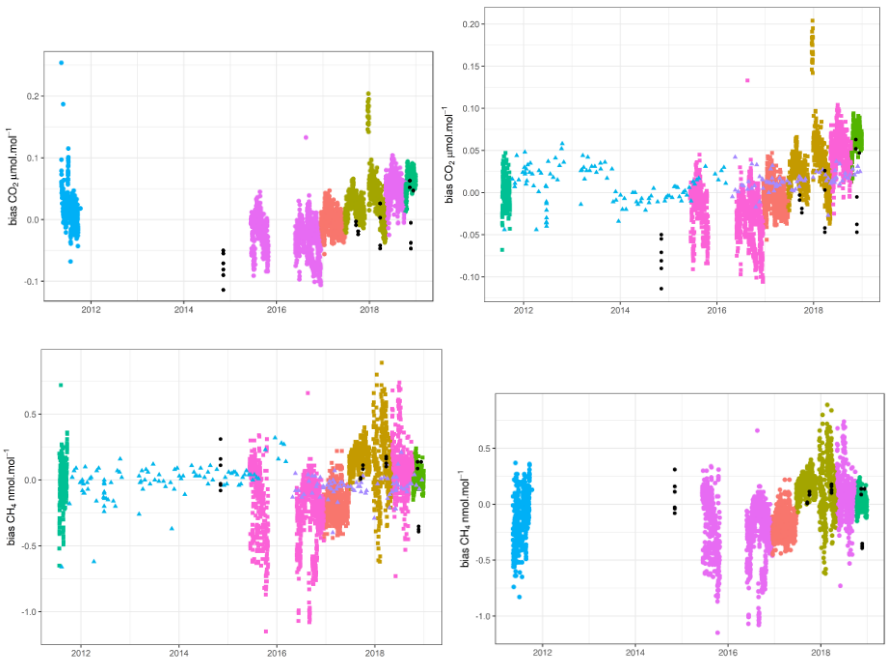
bias CO_2 µmol.mol^{-1}
bias CO_2 µmol.mol^{-1}
bias CH_4 nmol.mol^{-1}
bias CH_4 nmol.mol^{-1}
2012
2014
2016
2018

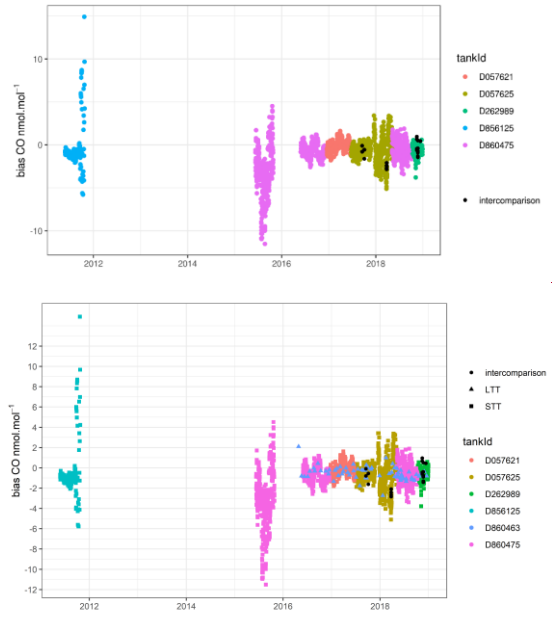

Figure 8~~7~~ Target tanks biases over time for several tanks for CO_2 (top left panel), CH_4 (top right panel) and CO (bottom panel) ~~in colours~~. The ~~The~~Short Term Target (STT), Long Term Target (LTT) and "~~c~~Cucumbers" intercomparison biases are shown in coloured squares, coloured triangles and black circle. The different colours are related to the different tanks used at the OPE station for quality control.

~~In addition the station OPE took part to the CarboEurope « cucumber » program in the EURO2 loop at the end of 2014, as well as to the ICOS program started in September 2017. The aims of such programs are to assess the measurement compatibility and quantify potential offsets in calibration scales within a network. The results of these two sequences of « cucumbers » intercomparison are shown on the Figure 7 along with the biases estimated for the station quality control cylinders.~~

~~The biases estimated from the target tanks operated at the station and the blind cucumber intercomparison biases are consistent for all species. CO_2 biases are found between -0.1 and 0.1ppm for most of the times except some outliers that still need to be understood. A trend may be present in the CO_2 biases between 2016 and 2018, not explained. CH_4 biases are between -0.75 and 0.75ppb for most of the cases. CO biases show a large spread at the beginning of the station operation partly related to the temperature sensitivity of the Los Gatos Research analyser and the poor temperature control of the measurements container. Since 2016 the CO biases stay within the -5 /+5 ppb range.~~

4. Results

Tall tower GHG mole fraction ~~concentration~~ time series over mid latitude~~s~~ continental areas exhibit strong variations from hours~~ly~~ to weeks, ~~seasons~~ seasonal and interannual time scales and even longer. Such variabilities are linked to local, regional and global meteorological variations, as well as land biosphere processes and human activities. ~~After~~ We will first show~~ing~~ the general characteristics of the time series. We will then analyse ~~, we will present~~and show the diurnal cycles computed from the despiked hourly data. We will ~~then~~ select only stable situations with low fast variability to ~~get a~~ focus on the regional scale and compute afternoon ~~stable~~ means for CO_2, CH_4, CO at the three sampling levels. The seasonal cycles and long-term trends will then be analysed and presented.

Mis en forme : Indice

Mis en forme : Indice

4.1 General characteristics of the CO_2, CH_4, and CO time~~s~~ series

~~The~~ Figure 9~~Figure 8~~ shows the general characteristics of the afternoon mean~~s measured~~ mole fractions ~~of~~ for CO_2, CH_4, CO at the OPE station at ~~the~~ 10m, 50m and 120 m above ground level~~s~~. ~~From the summer of 2011 to the end of 2018, the afternoon mean CO_2 at 120m varied from 375 ppm value to a maximum of 455 ppm. A higher variability is recorded at the lowest level (10m) compared to the top level (120m). At 10m the summer minimum concentrations are below the top level concentrations while the winter maximum concentrations are above the top level concentrations. Vertical gradients of CO_2 are present year round but are stronger in summer and weaker in winter, and the gradient variability is also much stronger in summer. During the warm period (from May to September) the mean vertical gradient of CO_2 is 0.4ppm during the afternoon (12:00-17:00 UTC) and -9.95 ppm during the night hours (00:00-05:00 UTC). During the cold period (from October to April) the mean vertical gradient of CO_2 is -0.24 ppm during the afternoon (12:00-17:00 UTC) and -3.5 ppm during the night hours (00:00-05:00 UTC). The CH_4 afternoon mean mole fractions time series are also characterized by a long term trend with a weaker seasonal cycle. Synoptic variations could be as large as 150 to 200 ppb on hourly time scales and are stronger at the lowest level. Vertical gradients of CH_4 are present year round and show a small seasonal cycle. During the warm period the mean vertical gradient of CH_4 is -0.5ppb during the afternoon (12:00-17:00 UTC) and -20.7 ppb during the night hours (00:00-05:00 UTC). During the cold period (from October to April) the mean vertical gradient of CH_4 is -4 ppb during the afternoon (12:00-17:00 UTC) and -18.5 ppb during the night hours (00:00-05:00 UTC).~~

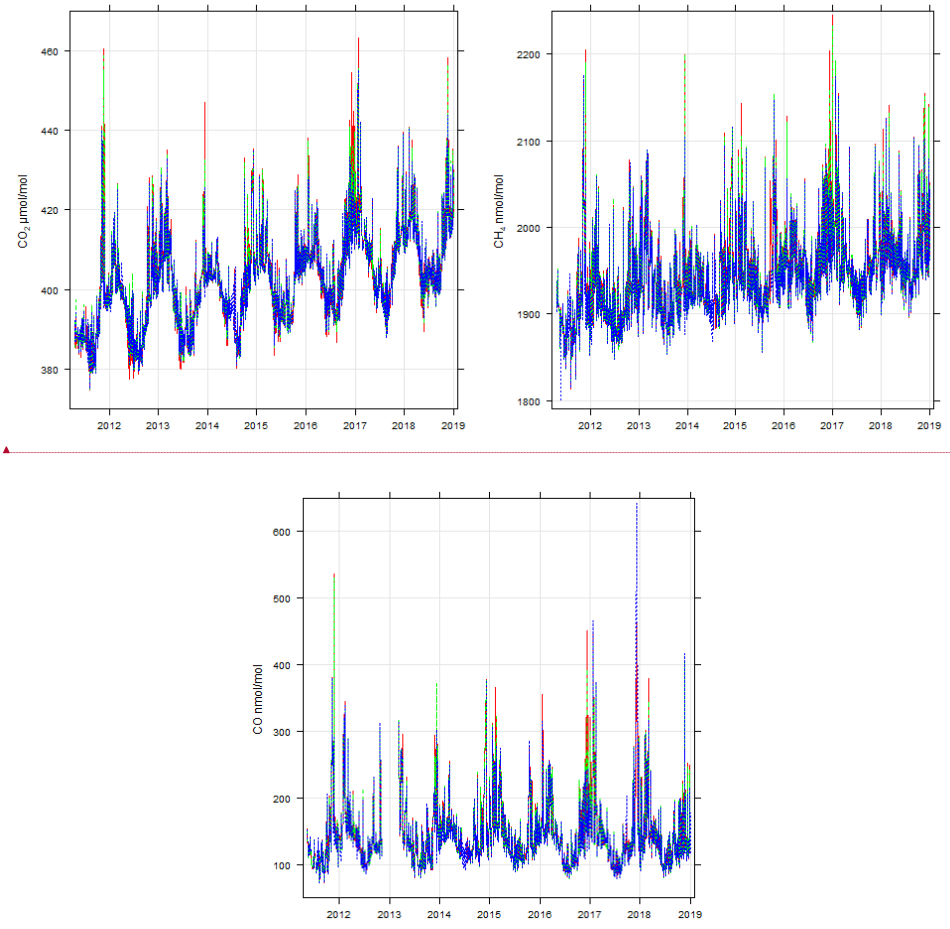

Figure 98: Afternoon (12:00-17:00 UTC) mean CO_2 (top left panel), CH_4 (top right panel) and CO (bottom panel) mole fractions measured at the OPE station at 10m (red), 50m (green) and 120m (blue).

From the summer of 2011 to the end of 2018, the afternoon mean CO_2 at 120m varied from 375 ppm to a maximum of 455 ppm. Over this seven year period, the afternoon mean time series show synoptic variations as well seasonal variations and interannual trends. Similar patterns were observed at several other long term monitoring stations in western Europe over

Mis en forme : Anglais (États-Unis)

different periods (Popa et al., 2010, Vermeulen et al., 2011, Schmidt et al., 2014, Lopez et al., 2014, Schibig et al., 2015, Satar et al., 2016, Stanley et al., 2018, Yuan et al., 2019). At European background stations such as the MHD coastal station or mountain stations (JFJ, Zugspitze-Schneefernerhaus ZSF or PDD) the interannual times series are dominated by long term trends and seasonal changes. At regional continental stations (CBW, TRN or Bialystok BIK), the synoptic variations have a much larger intensity due to the proximity of strong continental sources. The patterns and amplitude of synoptic variations and of seasonal changes depend on the sampling height, the lowest level (10m) having a higher variability than the highest level (120m). Vertical gradients of CO_2 are present year round but are stronger in summer and weaker in winter, and the gradient variability is much stronger in summer.

The time series forCH_4 afternoon mean mole fractions are also characterised by a long term trend with a weaker seasonal cycle. Synoptic variations can be as high as 150 to 200 ppb on hourly time scales and are stronger at the lowest level. Vertical gradients of CH_4 are present year round and show a small seasonal cycle. The time series CO afternoon mean mole fractions ~~time series~~ do not show any long-term trend~~s~~ but are characteri sed~~zed~~ by strong seasonal cycles. Synoptic variations ~~could~~ can be as ~~large~~ high as 200 ppb on hourly time scales and are stronger at the lowest level. Vertical gradients of CO are much stronger in winter and weaker in summer. ~~The CO lifetime in the atmosphere is strongly related to OH radicals, the major sink, which is seasonally variable. During summer the combined effects of a more active sink, weaker « local » sources and a strong vertical mixing lead to lower concentrations, with smaller variability and weaker vertical gradients. In winter, the OH sink efficiency decreases, local sources are stronger and the meteorological conditions favour non-dispersive situations and weaker vertical mixing leading to higher CO concentrations and stronger vertical gradients.~~

4.~~1~~ 2 Diurnal Cycles and vertical gradients

The ~~trace gases~~ diurnal cycles of trace gases ~~are the~~ result from~~s of the~~ atmospheric dynamics (especially the daily amplitude of the boundary layer height), ~~the~~ surface fluxes and ~~the~~ atmospheric chemistry. The mean diurnal cycles of CO_2, CH_4 and CO are shown ~~on the~~in Figure 10~~Figure 9~~ for the three sampling levels (10m, 50m and 120m). Despiked hourly data (not detrended or deseasonalised) were used to compute the mean diurnal cycles. CO_2, CH_4 and CO mole fractions displays similar diurnal cycles due to the similar atmospheric dynamics control: large increase of mean mole fractions and vertical gradient during night-time in contrast with a reduction of mean of mole fractions and vertical gradients during daytime. During the afternoon, while the CH_4 and CO mole fractions at the lowest level stay larger than those at the top level, the CO_2 mole fractions at the lowest level are slightly lower than those at higher level. This CO_2 depletion is due to vegetation ~~gowth~~growth and~~by~~ photosynthesis (which are stronger in summer and almost disappear in winter). ~~Lags are noticeable between the different levels in the CO_2 and CH_4 diurnal cycle. The night time peak concentrations occur earlier at the lowest level followed by the intermediate level and then followed by the highest level. The daytime minimum seems to be reached at the same time at the three levels. Then the late afternoon increase is much faster at the lowest level and is also delayed at the highest level.~~ The diurnal cycles of CO_2 and CH_4 are larger in spring and summer while for CO it is larger in winter.

Mis en forme : Indice
Mis en forme : Indice
Mis en forme : Indice
Mis en forme : Non Surlignage
Mis en forme : Indice
Mis en forme : Non Surlignage
Mis en forme : Indice, Non Surlignage
Mis en forme : Non Surlignage
Mis en forme : Non Surlignage
Mis en forme : Non Surlignage
Mis en forme : Non Surlignage

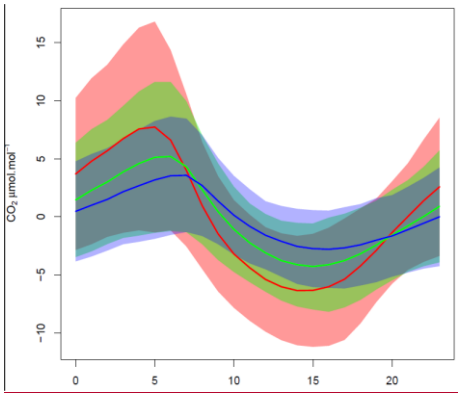
CO_2 µmol.mol^{-1}
15
10
5
0
−5
−10
0
5
10
15
20

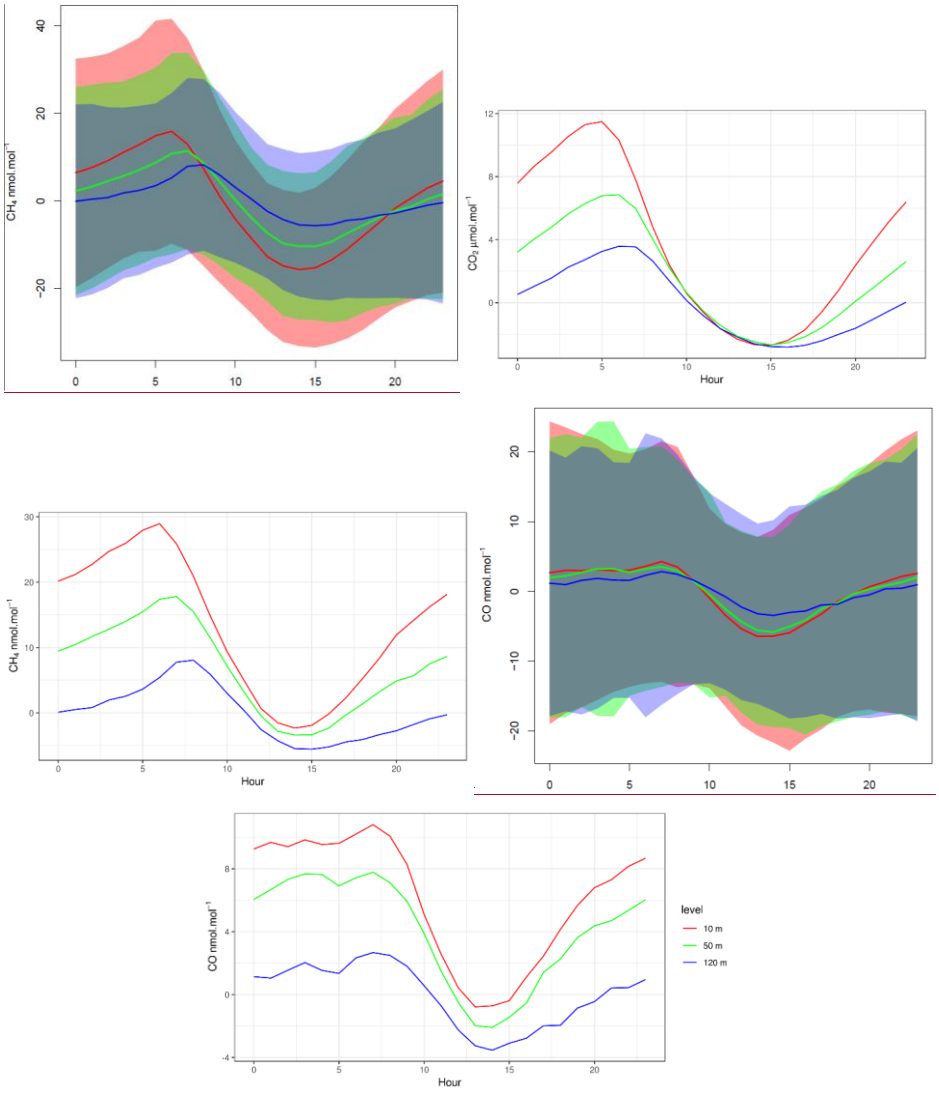
CH4 nmol.mol-1
CO2 µmol.mol-1
CH4 nmol.mol-1
CO nmol.mol-1
CO nmol.mol-1
Hour
level
10 m
50 m
120 m

Figure 109 Mean diurnal cycles of CO_2 (top left panel), CH_4 (top right panel) and CO (bottom panel) for the three sampling levels 10m (red), 50m (green) and 120m (blue), ~~normalized to the top level 120m,~~ computed over the period 2011-2018. The shaded areas correspond to the + and – 1 standard deviations around the mean diurnal cycles.

For the three compounds, the vertical gradients are much stronger ~~during the~~at night, and the highest mole fractions are measured near the ground~~with highest concentrations close to the ground~~. During the day~~time~~, the gradients almost disappear, mainly because of the ~~due to the~~enhanced vertical mixing of the lower atmosphere. In spring and summer, the ~~lowest level~~ CO_2 afternoon mole fraction at the lowest level ~~concentration~~ is slightly below that at the highest level reflecting the photosynthesis pumping of CO_2 by ~~the vegetation~~plants. Vertical CO_2 gradients build up again in the late afternoon. ~~For CH_4 and CO the vertical gradient stays the same all along the day, the lowest level being higher than the highest levels.~~

In the warm period (from May to September) the mean vertical gradient of CO_2 is 0.4 ppm during the afternoon (12:00-17:00 UTC) and -9.95 ppm at night (00:00-05:00 UTC). During the cold period (from October to April) the mean vertical gradient of CO_2 is -0.24 ppm during the afternoon (12:00-17:00 UTC) and -3.5 ppm at night (00:00-05:00 UTC). Similar patterns were observed at CBW, for the 1992 -2010 period but with stronger amplitude (Vermeulen et al., 2011). Stanley et al. (2018) showed the vertical gradients of CO_2 and CH_4 mole fractions at two tall towers in the United Kingdom (UK). Daytime vertical differences of CO_2 were very small (<1ppm) (positive in winter and negative in the other seasons). Night-time vertical gradients of CO_2 were always negative between 3 ppm and 8 ppm.

In the warm period the mean CH_4 vertical gradient is -0.5 ppb during the afternoon (12:00-17:00 UTC) and -20.7 ppb at night (00:00-05:00 UTC). In the cold period the mean CH_4 vertical gradient is -4 ppb during the afternoon and -18.5 ppb at night. Similar patterns and amplitudes were shown in the UK by Stanley et al. (2018). Vermeulen et al. (2011) also presented similar patterns but with larger amplitudes, the CBW vertical gradients of CH_4 reaching -300 ppb during summer between the 20m and 200m levels. .

~~Lags are noticeable between the different levels in the CO_2 and CH_4 diurnal cycle. The night-time peak concentrations occur earlier at the lowest level followed by the intermediate level and then followed by the highest level. The daytime minimum seems to be reached at the same time at the three levels. Then the late afternoon increase is much faster at the lowest level and is also delayed at the highest level. The diurnal cycles of CO_2 and CH_4 are larger in spring and summer while for CO it is larger in winter.~~

4.~~2~~ 3 Regional scale ~~Data~~signal extraction ~~selection and time series analysis~~

The station ~~hourly~~ time series exhibit strong variability from hourly to ~~decennial~~interannual time scales. These variations may be related to meteorological ~~and climate changes~~variability, and to variations in sources and sinks ~~variations~~. We are mostly interested in the regional signatures at scales that can be approached ~~by~~using ~~the~~ model inversions and assimilation ~~framework~~tools. For this reason we want to isolate ~~from the time series and data aggregation~~ the situations where the local influence is dominant and ~~is shadowing~~shadows the regional signature from the time series and data aggregation. We then need to define the background signal ~~on top of~~to which the regional scale signal is added.

Mis en forme : Indice
Mis en forme : Indice
Mis en forme : Indice
Mis en forme : Indice

Such local situations and background definitions may be extracted purely from time series analysis procedures, or may be constrained on a physical basis. ~~The main difficulty is to correctly define the baseline signal of the measured time series and to adequately flag local spikes.~~ El Yazidi et al. (2018) ~~have~~ assessed the efficiency and robustness of three statistical spikes detection methods for CO_2 and CH_4 and ~~have~~ concluded that the two automatic methods, namely Standard Deviations (SD) and Robust Extraction of Baseline Signal (REBS) ~~methods~~ could be used after a proper ~~parameters~~ specification of parameters. We used the El Yazidi et al. (2018) method on the composite merged minute time series to filter out « spike » situations. From ~~this~~the despiked minute data~~set~~ we built hourly means, which were used to analyse the diurnal cycles. Focusing on data with regional footprints, we selected only afternoon data with low hourly variability ~~(estimated from minute standard deviations)~~when the boundary layer is larger and the vertical mixing is more efficient. ~~–~~ We excluded data showing large variations by using the minute standard deviations. Hourly data with minute standard deviations larger than the three interquartile range computed month by month were excluded from the afternoon mean, leading to a rejection of 2.9 % to 4.2% of the hourly means of CO_2, CH_4 and CO. ~~We applied the CCGCRV curve fitting program from NOAA (Thoning et al., 1989) to determine the trend and the detrended seasonal cycle of the afternoon means time series for all species. Residuals from the trends and seasonal cycles were then computed.~~

~~Our aim in this paper is to draw the general behaviours of the major GHG at the station focusing on relatively large scale. We thus focused on stable data discarding situations when local influences could shadow the regional component. We selected afternoon data when the boundary layer is larger and the vertical mixing is more efficient as seen previously. We excluded data showing large variations by using the minute standard deviations. Hourly data with minute standard deviations larger than three interquartile range computed month by month were excluded from the afternoon mean, leading to a rejection of between 2.9 % and 4.2% of the hourly means of the CO_2, CH_4 and CO.~~

We then used the CCGCRV curve fitting program from NOAA (Thoning et al., 1989) with the standard parameters set (npoly=3, nharm=4) to compute the mean seasonal cycles and trends for the three compounds. CCGCRV results were compared with similar analysis performed ~~with~~ using the R package, ~~the o~~Openair ~~package~~(Carslaw and Ropkins, 2012) ~~of R~~ for the seasonal cycle and the trend using the Theil-~~S~~sen method (Sen, 1968). ~~These seasonal cycle and trend components of the time series are dominated by large scale processes. In addition strong intra-seasonal variabilities are observed that are related to local and regional scale factors~~. We then computed the afternoon mean residuals from the seasonal cycle and trends using the CCGCRV results. ~~We performed a qualitative comparison with residuals computed using the REBS approach which is commonly used to determine the station's background using a statistical approach (not shown). REBS was applied with a bandwidth of 60 days and a maximum of 20 iterations.~~

4.~~3~~ 4 Seasonal cycles

~~The~~ Figure 10 shows the mean seasonal cycles of ~~the three compounds~~ CO_2, CH_4 and CO at the three measurement levels (10m, 50m and 120m agl). Each of the three GHGs displays a clear seasonal cycle, with higher amplitudes at the lower

Code de champ modifié

sampling levels. Minimum values are reached during summer when the boundary layer is higher and the vertical mixing is more efficient. In addition to the boundary layer dynamics, the seasonal cycle of the surface fluxes and the chemical atmospheric sink also play ~~a~~ significant roles. The correlations of dynamic and fluxes~~s~~ processes at the seasonal scale make it difficult to ~~discriminate~~ distinguish the role of each process. CO_2 vertical gradients are observed in late autumn / early winter when the CO_2 mole fractions at 10m are larger than at 120m.

Mis en forme : Indice

Mis en forme : Indice

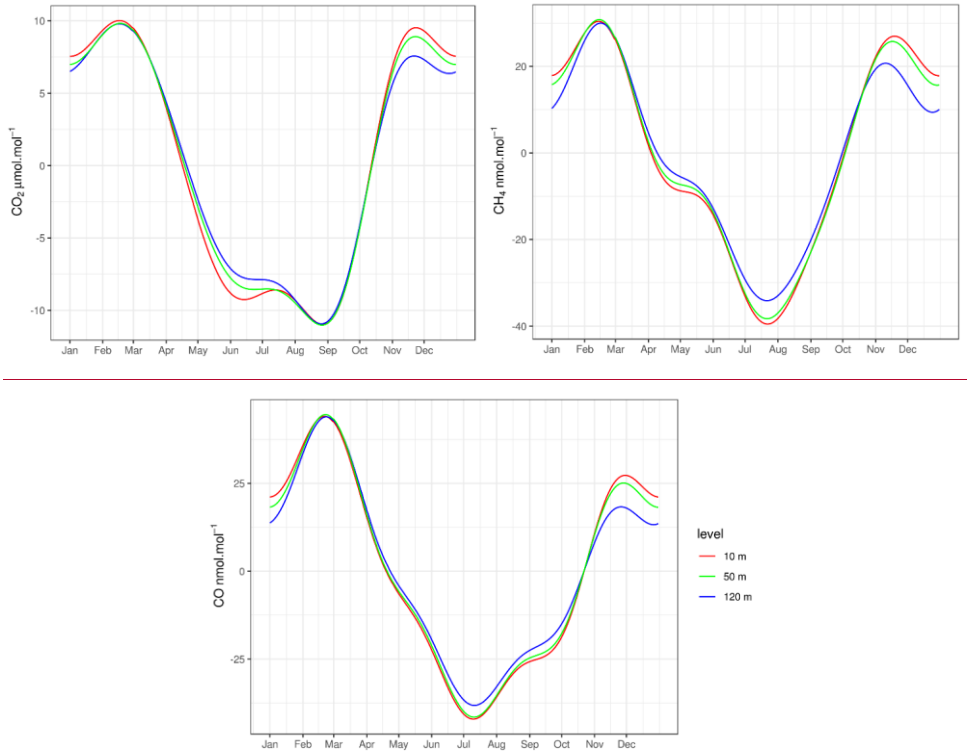

Figure 11:Mean seasonal cycles of the afternoon data at the three measurement levels (10m in red, 50m in green and 120m in blue) for CO_2 (top left panel), CH_4 (top right panel) and CO (bottom panel) computed over the 2011-2018 period using CCGCRV.

Minimum values are reached in late summer for CO_2, around the end of August with no vertical gradients around this minimum. Vertical gradients appear in ~~the~~ late spring with a maximum gradient in June when a secondary minimum is observed at the

lowest level but not at the ~~above~~ higher levels. The amplitude of the CO_2 seasonal cycle is nearly 21 ppm at the three levels. The CO_2 seasonal cycle amplitudes observed at BIK and CBW were between 25ppm and 30ppm depending on sampling height (Popa et al., 2010; Vermeulen et al., 2011). ~~CO_2 vertical gradients are also observed late fall - early winter when the lowest level CO_2 is higher than the top level.~~ The two early and late summer CO_2 minima were also observed by Haszpra et al. (2015), at the Hegyhatsal tall tower in western Hungary between 2006 and 2009, and their timings are very close to those of OPE. But only one summer minimum between August and September was observed at the BIK (Popa et al., 2010), CBW (Vermeulen et al., 2011) and TRN tall towers (Schmidt et al., 2014) and at the Schauinsland (SSL) and ZSF mountains stations (Yuan et al., 2019). Ecosystem CO_2 flux measurements performed in 2014 and 2015 near the OPE atmospheric station revealed that the forest and grassland Net Ecosystem Exchange had two maxima in early summer and late summer with a decrease in between (Heid et al., 2018). The two early and late winter maxima were also observed by Popa et al. (2010) at the BIK tall tower with similar timings , end of November and February. But only one winter maxima was observed in January at CBW (Vermeulen et al., 2011), TRN (Schmidt et al., 2014) and Hegyhatsal (Haszpra et al., 2015), in February at SSL and in March at the ZSF mountain station (Yuan et al., 2019).

Mis en forme : Indice

Mis en forme : Indice

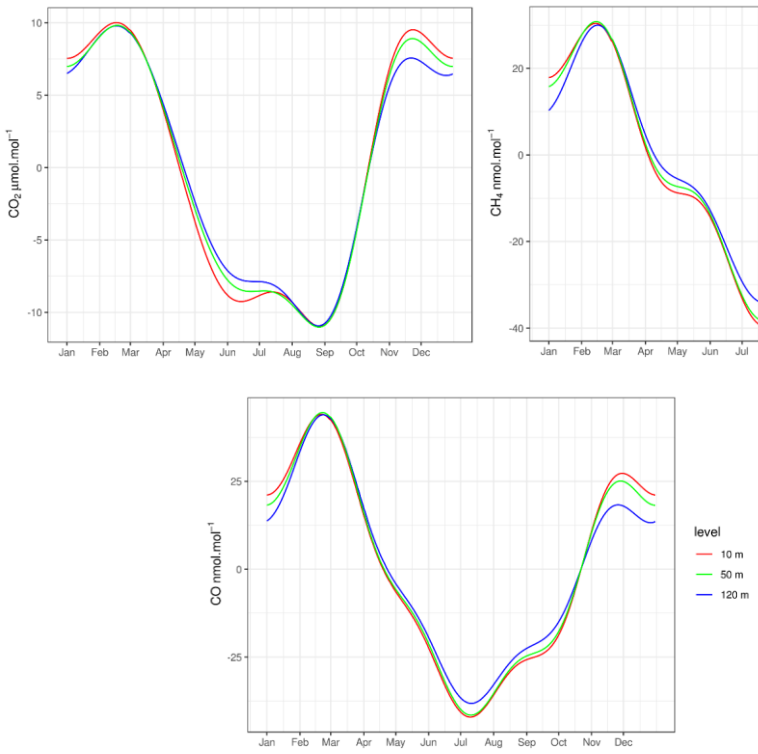

~~**Figure 10:Mean seasonal cycles of the afternoon mean data at the three measurement levels (10m in red, 50m in green and 120m in blue) for CO_2 (top left panel), CH_4 (top right panel) and CO (bottom panel) computed over the 2011-2018 period using CCGCRV.**~~

At OPE ~~M~~minimum CH_4 values are observed- in July and maximum values are reached ~~values~~ in February and November. The peak-to-peak amplitude of the CH_4 seasonal cycle is nearly 70 ppb at the three levels. ~~The vertical gradients of CH_4 are stronger in mid-summer and early winter compared to the other seasons.~~ At BIK, there was only one maximum in December and minimum values were reached between May and June (Popa et al., 2010). The seasonal cycle amplitude was between 64 and 88 ppb. At CBW, CH_4 mole fractions peaked at the end of December and were at minimum at the end of August. The seasonal cycle amplitude was between 50 ppb and 110 ppb depending on the sampling level (Vermeulen et al., 2011).

The CO seasonal cycle peaks at the end of February, with a secondary peak at the end of November. Minimum values are reached in July, earlier than the CO_2 and CH_4 minimum. The peak-to-peak amplitude of the CO seasonal cycle is between 80ppb and 90ppb. At BIK, the CO maximum was reached in January (with a delay compared to CO_2 and CH_4) and minimum

Mis en forme : Indice

Mis en forme : Indice

Mis en forme : Indice

Mis en forme : Indice

values were observed in June, with a peak to peak seasonal cycle amplitude between 130ppb and 200ppb (Popa et al., 2010). At CBW, the CO maximum was reached in January (also with a delay compared to CO_2 and CH_4) and minimum values were observed in August. The peak to peak CO seasonal cycle amplitude varied between 90ppb and 130ppb (Vermeulen et al., 2011).~~The CO vertical gradients are maximum in November and December. This highlights the enhanced winter anthropogenic emission associated with heating as well as the reduced atmospheric mixing. Large-scale transport may contribute to the increase as emission increases in winter on continental scale. But local activities are also contributing as shown by the stronger vertical gradients and the higher mole fraction levels near the ground. CO_2 vertical gradients are stronger in November and December, as also shown in the CH_4 and CO vertical gradients, and are weaker from January to April.~~

Mis en forme : Indice

Mis en forme : Indice

4.~~4~~ 5 Trends

~~The~~ Table 7~~Table 6~~ reports the mean atmospheric growth rates computed for the three compounds at the top level using the CCGCRV and Theil-Ssen approaches. The ~~M~~mean annual growth rate of CO_2 ~~annual growth rate~~ over the 2011-2018 period is 2.5 ppm/year using the Theil-Ssen method and 2.3 ppm/year using CCGCRV. This is ~~in agreement~~consistent ~~-~~with the Mauna Loa global station rate which is also 2.4 ppm/year on average for the period 2011-2018. It is stronger than the growth rate reported for the ~~Zugspitze~~ ZSF mountain ~~site~~station: 1.8ppm /year, ~~for~~ over 1981-2016 (Yuan et al., 2019), ~~as well as~~and for the ~~Cabauw~~CBW station: 2.0 ppm/year, over 2005-2009 (Vermeulen et al., 2011). Such comparisons are only qualitative and must be used with caution, as the time periods considered are different. However, they suggest that the atmospheric CO_2 growth may speed up in the European mid-latitudes.

Mis en forme : Indice

~~The mean CH_4 annual growth rate over the 2011-2018 period is 8.8 ppb/year using CCGCRV and 8.9 ppb/year using Theilsen method. It is a bit larger than the annual increase in Globally-Averaged Atmospheric Methane from NOAA which is 7.5 ppb /year over the 2011-2017 period. The CO shows a slightly decreasing non-significant trend at OPE for the period 2011-2018. This finding is consistent with recent observations in Europe and in the US. After a long global decrease since the 1980's, the CO decrease has declined since several years after reaching values below 2 ppm (Lowry et al., 2016, Zellweger et al. 2016).~~

OPE-120m	CO_2 (ppm)	CH_4 (ppb)	CO (ppb)
CCGCRV 2011-2018	2.~~32~~35 (1.93 ;2.77)	8.~~83~~85 (7.35 ; 10.34)	-0.22 (-3.9 ; 3.5)~~4~~
Theil-Ssen2011-2018	2.~~48~~54 (1.92 ; 3.28)	8.~~86~~91 (7.64 ;9.96)	-0.~~37~~49 (-1.71 ;0.73)

Table ~~7~~6: Growth rates of CO_2, CH_4 and CO mole fractions at OPE 120m level for the period 2011-2018 computed on the afternoon mean data using the CCGCRV and Theil-Ssen methods. 95% confidence intervals are displayed for each compound and method.

The OPE mean CH_4 annual growth rate over the 2011-2018 period is 8.8 ppb/year using CCGCRV and 8.9 ppb/year using the Theil-Sen method. It is slightly larger than the annual increase in Globally-Averaged Atmospheric Methane from NOAA which is 7.5 ppb /year over the 2011-2017 period. A slightly decreasing non-significant trend is seen for CO at OPE over the

Mis en forme : Normal

2011-2018 period. This finding is consistent with recent observations in Europe and in the US. After a global decrease since the end of the 1980s, CO decrease has declined for several years after reaching values below 0.2 ppm at some European background sites such as MHD or JFJ (Lowry et al., 2016, Novelli et al., 2003; Zellweger et al., 2009).

4.~~5~~6 CO_2, CH_4 and CO residuals

We analysed the120m level residuals from the trend and seasonal cycle~~s~~ fitted curves with regard~~s~~ to air masses back-trajectories using the six clusters defined for the afternoon ~~back trajectories~~ (see Figure 2~~Figure 2~~). ~~The~~ Figure 11 shows the boxplots of the residuals for each month and back-trajectories cluster. The boxplot displays the first and third quartile and the median of the residuals ~~as well as~~along with the overall data extension.

Code de champ modifié

cluster	1		2		3		4		5		6	
period	warm	cold	warm	cold	warm	cold	warm	cold	warm	cold	warm	cold
CO_2 / CH_4	0.21	0.92	0.33	0.89	0.01	0.84	0.47	0.86	0.18	0.8	0.24	0.87
CO_2 / CO	0.16	0.91	0.4	0.87	0.24	0.85	0.52	0.91	0.24	0.74	0.24	0.78
CH_4 / CO	0.74	0.93	0.87	0.84	0.71	0.87	0.76	0.92	0.75	0.85	0.78	0.88

Table 8 Correlation coefficients between the compounds residuals for each cluster, split between a warm period from April to September and a cold period from October to March.

The residuals of the three compounds are significantly stronger in the cold months than ~~during~~ in the warm months. ~~The c~~Clusters 5 (shown in blue ~~colour in Figure 11~~) and 6 (in cyan) are associated with typical oceanic air masses with 96 hour back-trajectories reaching far over the Atlantic Ocean. ~~Such~~ These air masses are associated with the ~~smallest~~ lowest ~~residuals~~ variability of residuals (smallest boxplot extension). Negative residuals are noticed year-round for CH_4 and CO and during the cold months for CO_2 (positive during warm months). Clusters 1 (brown) and 2 (red) are associated with southern and eastern trajectories. The associated residuals are much stronger and show large variabilities among the different synoptic situations with potential large deviations from the background.

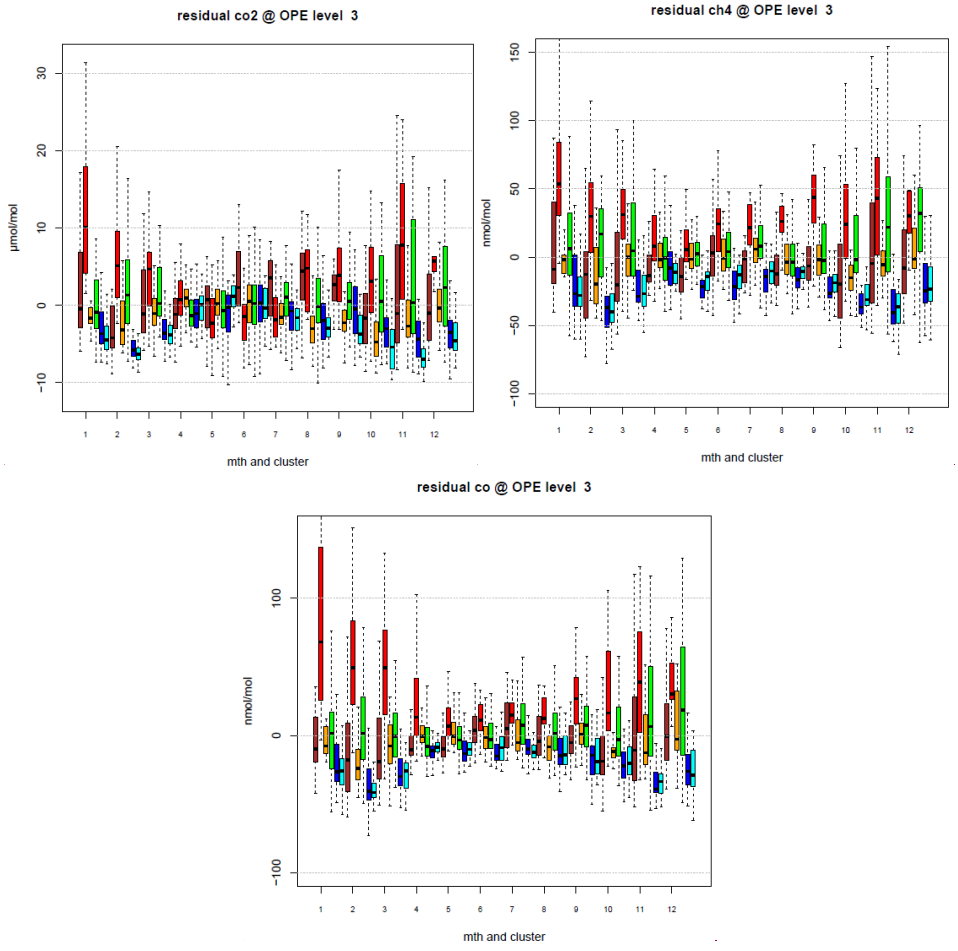

~~**Figure 11: Seasonal boxplot of the CO_2 (top left panel), CH_4 (top right panel) and CO residuals (bottom panel) at OPE by cluster occurrence (cluster 1: brown, cluster 2 : red, cluster 3 : orange, cluster 4 : green, cluster 5 : blue, cluster 6 : cyan) for the period 2011-2018**~~

~~Positive residuals are noticed for cluster 2 year-round for CH_4 and CO and during the cold months for CO_2. Cluster 3 (orange) is associated with neutral residuals either negative or positive for the three compounds. Cluster 4 (green) is characterised by relatively "stagnant " air masses with back-trajectories that do not extend far from the station in any particular directions. This~~

Mis en forme : Indice

Mis en forme : Indice

type of air masses is associated with large residuals variability for the three compounds during the cold months. The residuals can be either positive or negative and show large spreads among the situations.

The Table 7 shows the correlation coefficients between the compounds residuals for each back-trajectories cluster, split between a warm period from April to September and a cold period from October to March. During the warm period, the correlation coefficients between CO_2 and either CH_4 or CO are low except for cluster 4. However, the correlation coefficients between CH_4 and CO are around 0.75 for each cluster. During the cold period, the correlation coefficients between the different compounds are high and significant for every type of back-trajectories. Similar seasonal pattern of the CO_2/CO residuals and CO/CH_4 residuals were shown by Satar et al. (2016) in their two years analysis of the Beromunster tower data in Switzerland.

cluster	1		2		3		4		5		6	
period	warm	cold	warm	cold	warm	cold	warm	cold	warm	cold	warm	cold
CO_2 / CH_4	0.21	0.92	0.33	0.89	0.01	0.84	0.47	0.86	0.18	0.8	0.24	0.87
CO_2 / CO	0.16	0.91	0.4	0.87	0.24	0.85	0.52	0.91	0.24	0.74	0.24	0.78
CH_4 / CO	0.74	0.93	0.87	0.84	0.71	0.87	0.76	0.92	0.75	0.85	0.78	0.88

Table 7 Correlation coefficients between the compounds residuals for each cluster, split between a warm period from April to September and a cold period from October to March.

Mis en forme : Normal

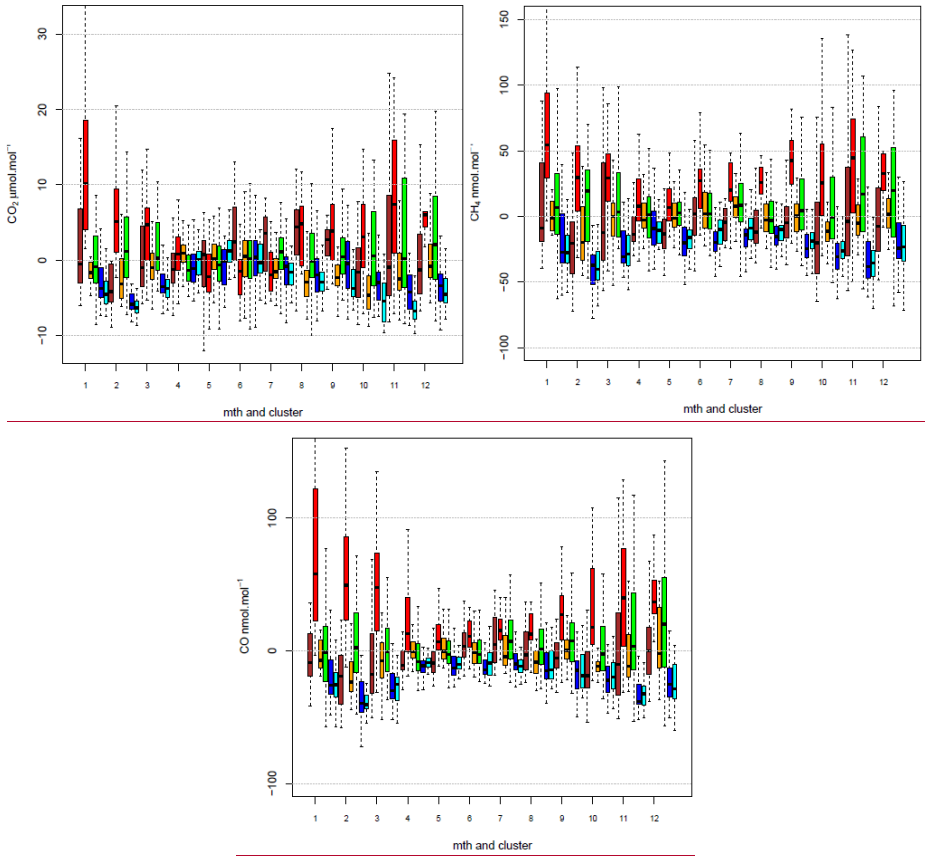

Figure 12: Seasonal boxplot of the CO_2 (top left panel), CH_4 (top right panel) and CO residuals (bottom panel) at OPE 120m levels by cluster occurrence (cluster 1: brown, cluster 2 : red, cluster 3 : orange, cluster 4 : green, cluster 5 : blue, cluster 6 : cyan) for the period 2011-2018

Positive residuals are associated with Cluster 2 year-round for CH_4 and CO and during the cold months for CO_2. Cluster 3 (orange) is associated with either negative or positive residuals for the three compounds. Cluster 4 (green) is characterised by relatively "stagnant " air masses with back-trajectories that do not extend far from the station in any particular directions. This type of air mass is associated with high residuals variability for the three compounds during the cold period. The residuals can be either positive or negative and show large spreads among the situations.

shows the correlation coefficients between the compounds residuals for each back-trajectory cluster, split between a warm period from April to September and a cold period from October to March. During the warm period, the correlation coefficients between CO_2 and either CH_4 or CO are low except for Cluster 4. However, the correlation coefficients between CH_4 and CO are around 0.75 for each cluster. During the cold period, the correlation coefficients between the different compounds are high and significant for every type of back-trajectory. Similar seasonal patterns for the CO_2/CO residuals and CO/CH_4 residuals were shown by Satar et al. (2016) in their two-year analysis of the Beromunster tower data in Switzerland.

Mis en forme : Normal

Such patterns suggest that, during the cold months, the variations of three compounds ~~fluctuations~~ are associated with the same anthropogenic processes convoluted through ~~the~~ atmospheric dispersion. However, during the warm months, intraseasonal variations CO_2 residuals ~~intraseasonal variations~~ may have different drivers than CO or CH_4 residuals or their scale footprints are different. For example, natural biospheric contributions from different scales (local to continental) are larger for CO_2 during the warm months. Photochemical reactions are also much more activated during summertime. This result ~~is suggesting~~ suggests that biospheric CO_2 fluxes may be the dominant driver of CO_2 intraseasonal variations during the warm period while anthropogenic emissions ~~are~~ lead~~ing~~ the intraseasonal variations of the three compounds during the cold period.

5. Conclusion

The OPE station is a new atmospheric station that was set up in 2011 as part of the ICOS Demo Experiment. It is a continental station sampling regionally representative air-masses ~~influenced within regional footprints~~. In addition to greenhouse gases and meteorological parameters mandatory for ICOS, the station ~~is measuring~~measures aerosol properties~~,~~ and radioactivity and is part of the regional air quality network. The ~~greenhouse gases~~GHG measurements are performed in compliance with the ICOS atmospheric station specifications, and ~~it~~ the station was labelled ~~as part of~~by ICOS ~~ERIC~~ in 2017. We have presented the GHG measurement system as well as the quality control performed. ~~Then~~ Next, analysis of the diurnal cycles, seasonal cycles and trends were ~~shown~~ given for the GHG data over the ~~period~~ 2011-2018 period. ~~Lastly~~ Finally; we analysed the compounds residuals with regard~~s~~ to the air masse~~s~~ history.

The monthly mean field CMRs were estimated at between 0.01 and 0.04 ppm for CO_2, 0.14 and 0. 5 ppb for CH_4 and 0.1 and 5.4 ppb for CO. The monthly mean field LTRs were estimated at between 0.003 and 0.013 ppm for CO_2, between 0.03 and 0.23 ppb for CH_4, and between 0.14 and 2.17ppb for CO. Biases estimated from the station working standards or by the "C~~e~~ucumbers" intercomparison ~~are~~ have been between ±0.1 ppm for CO_2, ±0.75 ppb for CH_4 and ±5 ppb for CO since 2016. The station was audited ~~two times~~twice, ~~once~~ just after its ~~start~~ launch in 2011 and then in 2014. In 2011, the field audit revealed a median difference of 0.13 ppm for CO_2 and of 0.4 ppb for CH_4. During the 2014 audit, the mean biases were between 0.03 and 0.05 ppm for CO_2 and between 0.7 and 1.8 ppb for CH_4. The audits results along with the routine quality control metrics such as CMR, LTR and biases, and the "Cucumbers" intercomparisons showed that the OPE station met the

compatibility goals defined by the WMO for CO_2, CH_4, and CO most of the time between 2011 and 2018 (WMO, 2018). The station set-up and its standard operating procedures are also fully compliant with the ICOS specifications (Laurent et al.,. 2017).

The diurnal cycles of the three compounds show ~~the~~ amplification of the vertical gradient ~~during at~~~~the~~ night mainly caused by the night-time boundary layer stratification associated with ~~the~~ ground cooling and ~~the~~ radiative loss. Minimum values are reached during the afternoon ~~daytime~~ when ~~the~~ vertical mixing is more efficient. In addition to this main atmospheric dynamics influence, diurnal cycles of ~~the~~ surface emissions and of ~~the~~ photochemical processes ~~are~~ also play~~ing~~ some roles in the diurnal profiles of the three compounds~~. Interested on larger scale processes~~. ~~w~~We focused on the afternoon data as we are interested in larger scale processes. We computed the mean seasonal cycles of CO_2, CH_4 and CO. In addition ~~quite~~ relatively strong positive trends were observed for CO_2 and CH_4 with a mean annual growth rate of 2.4 ppm/year and 8.8 ppb/year respectively for the period 2011-2018. No significant trend was observed for CO.

The residuals from the trends and seasonal cycles ~~identified by the time series decompositions~~ are much stronger during the cold period (October to March) than during the warm period (April to September~~r~~.). Our analysis of the residuals highlights the major influence of ~~the~~ air masses on the atmospheric composition~~s~~ residuals. Air masses originating from the western quadrant with an Atlantic Ocean signature are associated with the lowest residual variability. Eastern continental air masses or stagnant situations are associated with larger residuals and ~~large~~ high variability. The correlations between the compounds residuals are also stronger during the cold period. Furthermore, there are no significant correlation between CO_2 and CO or CH_4 during the warm period.~~. This is reflecting that summer CO_2 residuals have important natural sources while anthropogenic drivers dominate CO and CH_4 variations.~~

Mis en forme : Indice

Acknowledgements

The authors gratefully acknowledge the NOAA Air Resources Laboratory (ARL) for the provision of the HYSPLIT transport and dispersion model and~~/or~~ READY website (http://www.ready.noaa.gov) used in this publication. S. Hammer from Heidelberg University and H. Aaltonen from FMI are thanked for their efforts during the OPE station audits. Staff from IRFU-CEA are acknowledged for their contribution to the station's initial design and installation. We also thank staff from SNO-ICOS-France and from the ICOS Atmospheric Thematic Center for their technical support. The authors would like to thank the editor and two anonymous referees who provided valuable suggestions and constructive comments to improve the manuscript.

Competing interests: The authors declare that they have no conflict of interest.

References

Bergamaschi, P., Karstens, U., Manning, A. J., Saunois, M., Tsuruta, A., Berchet, A., Vermeulen, A. T., Arnold, T., Janssens-Maenhout, G., Hammer, S., Levin, I., Schmidt, M., Ramonet, M., Lopez, M., Lavric, J., Aalto, T., Chen, H., Feist, D. G., Gerbig, C., Haszpra, L., Hermansen, O., Manca, G., Moncrieff, J., Meinhardt, F., Necki, J., Galkowski, M., O'Doherty, S., Paramonova, N., Scheeren, H. A., Steinbacher, M., and Dlugokencky, E.: Inverse modelling of European CH4 emissions during 2006–2012 using different inverse models and reassessed atmospheric observations, Atmos. Chem. Phys., 18, 901-920, https://doi.org/10.5194/acp-18-901-2018, 2018

Berhanu, T. A., Satar, E., Schanda, R., Nyfeler, P., Moret, H., Brunner, D., Oney, B., and Leuenberger, M.: Measurements of greenhouse gases at Beromünster tall-tower station in Switzerland, Atmos. Meas. Tech., 9, 2603-2614, https://doi.org/10.5194/amt-9-2603-2016, 2016

Broquet, G., Chevallier, F., Bréon, F.-M., Kadygrov, N., Alemanno, M., Apadula, F., Hammer, S., Haszpra, L., Meinhardt, F., Morguí, J. A., Necki, J., Piacentino, S., Ramonet, M., Schmidt, M., Thompson, R. L., Vermeulen, A. T., Yver, C., and Ciais, P.: Regional inversion of CO2 ecosystem fluxes from atmospheric measurements: reliability of the uncertainty estimates, Atmos. Chem. Phys., 13, 9039-9056, https://doi.org/10.5194/acp-13-9039-2013, 2013.

Carslaw DC, Ropkins K : openair — An R package for air quality data analysis. Environmental Modelling & Software, 27–28(0), 52–61, 2012

El Yazidi, A., Ramonet, M., Ciais, P., Broquet, G., Pison, I., Abbaris, A., Brunner, D., Conil, S., Delmotte, M., Gheusi, F., Guerin, F., Hazan, L., Kachroudi, N., Kouvarakis, G., Mihalopoulos, N., Rivier, L., and Serça, D.: Identification of spikes associated with local sources in continuous time series of atmospheric CO, CO_2 and CH_4, Atmos. Meas. Tech., 11, 1599-1614, https://doi.org/10.5194/amt-11-1599-2018, 2018.

Hammer, S., Konrad, G., Vermeulen, A. T., Laurent, O., Delmotte, M., Jordan, A., Hazan, L., Conil, S., and Levin, I.: Feasibility study of using a "travelling" CO_2 and CH_4 instrument to validate continuous in situ measurement stations, Atmos. Meas. Tech., 6, 1201-1216, https://doi.org/10.5194/amt-6-1201-2013, 2013

Hazan, L., Tarniewicz, J., Ramonet, M., Laurent, O., and Abbaris, A.: Automatic processing of atmospheric CO_2 and CH_4 mole fractions at the ICOS Atmosphere Thematic Centre, Atmos. Meas. Tech., 9, 4719-4736, https://doi.org/10.5194/amt-9-4719-2016, 2016

Mis en forme : Anglais (États-Unis)

Heid, L., Calvaruso, C., Andrianantenaina, A. Granier A., Conil S., Rathberger C., Turopault M.P., Longdoz B. : Seasonal time-course of the above ground biomass production efficiency in beech trees (Fagus sylvatica L.). Annals of Forest Science 75: 31. https://doi.org/10.1007/s13595-018-0707-9, 2018

Kadygrov, N., Broquet, G., Chevallier, F., Rivier, L., Gerbig, C., and Ciais, P.: On the potential of the ICOS atmospheric CO_2 measurement network for estimating the biogenic CO_2 budget of Europe, Atmos. Chem. Phys., 15, 12765-12787, https://doi.org/10.5194/acp-15-12765-2015,

Kountouris, P., Gerbig, C., Rödenbeck, C., Karstens, U., Koch, T. F., and Heimann, M.: Atmospheric CO_2 inversions on the mesoscale using data-driven prior uncertainties: quantification of the European terrestrial CO_2 fluxes, Atmos. Chem. Phys., 18, 3047-3064, https://doi.org/10.5194/acp-18-3047-2018, 2018

Kromer B., Münnich K.O.: ~~Co2~~ CO_2 Gas Proportional Counting in Radiocarbon Dating — Review and Perspective. In: Taylor R.E., Long A., Kra R.S. (eds) Radiocarbon After Four Decades. Springer, New York, NY,1992

Laurent, O.: ICOS Atmospheric Station Specifications, ICOS technical report (publicly available on https://icos-atc.lsce.ipsl.fr/doc_public), 2017

Le Quéré, C. and coauthors: Global Carbon Budget 2018, Earth System Science Data, 10, 1-54, 2018, DOI: 10.5194/essd-10-2141-2018

Lebegue, B., Schmidt, M., Ramonet, M., Wastine, B., Yver Kwok, C., Laurent, O., Belviso, S., Guemri, A., Philippon, C., Smith, J., and Conil, S.: Comparison of nitrous oxide (N_2O) analyzers for high-precision measurements of atmospheric mole fractions, Atmos. Meas. Tech., 9, 1221-1238, https://doi.org/10.5194/amt-9-1221-2016, 2016

Leip A, Skiba U, Vermeulen A, Thompson RL.:. A complete rethink is needed on how greenhouse gas emissions are quantified for national reporting. Atmospheric Environment. 174:237-240. https://doi.org/10.1016/j.atmosenv.2017.12.006; 2018

Levin, I., Münnich, K., Weiss, W.: The Effect of Anthropogenic CO_2 and 14C Sources on the Distribution of 14C in the Atmosphere. Radiocarbon, 22(2), 379-391. doi:10.1017/S003382220000967X,1980

Lopez, M., Schmidt, M., Ramonet, M., Bonne, J.-L., Colomb, A., Kazan, V., Laj, P., and Pichon, J.-M.: Three years of semicontinuous greenhouse gas measurements at the Puy de Dôme station (central France), Atmos. Meas. Tech., 8, 3941-3958, https://doi.org/10.5194/amt-8-3941-2015, 2015

Mis en forme : Anglais (États-Unis)
Mis en forme : Anglais (États-Unis)
Mis en forme : Indice
Mis en forme : Indice
Mis en forme : Indice

~~Lowry, D. et al.~~

Lowry D., Lanoisellé M.E., Fisher R. E., Martin M., Fowler C. M. R., France J. L., Hernández-Paniagua1 I. Y., Novelli P.C., Sriskantharajah S., O'Brien P., Rata N.D., Holmes C.W., Fleming Z. L., Clemitshaw K. C., Zazzeri G., Pommier M., McLinden C. A. and Nisbet E.G.: Marked long-term decline in ambient CO mixing ratio in SE England, 1997–2014: evidence of policy success in improving air quality. Sci. Rep. 6, 25661; doi: 10.1038/srep25661, 2016

Nisbet, E. G., Manning, M. R., Dlugokencky, E. J., Fisher, R. E., Lowry, D., Michel, S. E., et al: Very strong atmospheric methane growth in the 4 years 2014–2017: Implications for the Paris Agreement. Global Biogeochemical Cycles, 33. https://doi.org/10.1029/2018GB006009, 2019

Novelli, P. C., Masarie, K. A., Lang, P. M., Hall, B. D., Myers, R. C., and Elkins, J. W. (2003), Reanalysis of tropospheric CO trends: Effects of the 1997–1998 wildfires, J. Geophys. Res., 108, 4464, doi:10.1029/2002JD003031, D15

Peters, G. P., Le Quéré, C., Andrew, R. M., Canadell, J. G., Friedlingstein, P., Ilyina, T., Jackson, R. B., Joos, F., Korsbakken, J. I., McKinley, G. A., Sitch, S., and Tans, P.: Towards real-time verification of CO_2 emissions, Nat. Clim. Change, 7, 848–850, https://doi.org/10.1038/s41558-017-0013-9, 2017

Pison, I., Berchet, A., Saunois, M., Bousquet, P., Broquet, G., Conil, S., Delmotte, M., Ganesan, A., Laurent, O., Martin, D., O'Doherty, S., Ramonet, M., Spain, T. G., Vermeulen, A., and Yver Kwok, C.: How a European network may help with estimating methane emissions on the French national scale, Atmos. Chem. Phys., 18, 3779-3798, https://doi.org/10.5194/acp-18-3779-2018, 2018

Rella, C. W., Chen, H., Andrews, A. E., Filges, A., Gerbig, C., Hatakka, J., Karion, A., Miles, N. L., Richardson, S. J., Steinbacher, M., Sweeney, C., Wastine, B., and Zellweger, C.: High accuracy measurements of dry mole fractions of carbon dioxide and methane in humid air, Atmos. Meas. Tech., 6, 837-860, https://doi.org/10.5194/amt-6-837-2013, 2013

Satar, E., Berhanu, T. A., Brunner, D., Henne, S., and Leuenberger, M.: Continuous CO_2/CH_4/CO measurements (2012–2014) at Beromünster tall tower station in Switzerland, Biogeosciences, 13, 2623-2635, https://doi.org/10.5194/bg-13-2623-2016, 2016

Mis en forme : Indice

Schibig, M. F., Steinbacher, M., Buchmann, B., van der Laan-Luijkx, I. T., van der Laan, S., Ranjan, S., and Leuenberger, M. C.: Comparison of continuous in situ CO_2 observations at Jungfraujoch using two different measurement techniques, Atmos. Meas. Tech., 8, 57-68, https://doi.org/10.5194/amt-8-57-2015, 2015

Schmidt, M., Lopez, M., Yver Kwok, C., Messager, C., Ramonet, M., Wastine, B., Vuillemin, C., Truong, F., Gal, B., Parmentier, E., Cloué, O., and Ciais, P.: High-precision quasi-continuous atmospheric greenhouse gas measurements at Trainou tower (Orléans forest, France), Atmos. Meas. Tech., 7, 2283-2296, https://doi.org/10.5194/amt-7-2283-2014, 2014

Sen, P.K.: Estimates of the regression coefficient based on Kendall's tau, Journal of the American Statistical Association, 63 (324): 1379–1389, doi:10.2307/2285891, 1968.

Thoning, K.W., P.P. Tans, and W.D. Komhyr, Atmospheric carbon dioxide at Mauna Loa Observatory, 2. Analysis of the NOAA/GMCC data, 1974 1985., J. Geophys. Res. ,94, 8549 8565,1989

Vardag, S. N., Hammer, S., O'Doherty, S., Spain, T. G., Wastine, B., Jordan, A., and Levin, I.: Comparisons of continuous atmospheric CH_4, CO_2 and N_2O measurements – results from a travelling instrument campaign at Mace Head, Atmos. Chem. Phys., 14, 8403-8418, https://doi.org/10.5194/acp-14-8403-2014, 2014

Turner, A.J., Frankenberg, C., Kort, E.A.: Interpreting contemporary trends in atmospheric methane, Proc. Natl. Acad. Sci., 116 (8) 2805-2813; DOI: 10.1073/pnas.1814297116, 2019

Vermeulen, A. T., Hensen, A., Popa, M. E., van den Bulk, W. C. M., and Jongejan, P. A. C.: Greenhouse gas observations from Cabauw Tall Tower (1992–2010), Atmos. Meas. Tech., 4, 617-644, https://doi.org/10.5194/amt-4-617-2011, 2011

WMO: 19th WMO/IAEA Meeting on Carbon Dioxide, Other Greenhouse Gases and Related Tracers Measurement Techniques (GGMT-2017), Dübendorf, Switzerland, 27-31 August 2017, GAW Report No.242, World Meteorological Organization, Geneva, Switzerland, 2018

Yuan, Y., Ries, L., Petermeier, H., Trickl, T., Leuchner, M., Couret, C., Sohmer, R., Meinhardt, F., and Menzel, A.: On the diurnal, weekly, and seasonal cycles and annual trends in atmospheric CO2 at Mount Zugspitze, Germany, during 1981–2016, Atmos. Chem. Phys., 19, 999-1012, https://doi.org/10.5194/acp-19-999-2019, 2019

Yver Kwok, C., Laurent, O., Guemri, A., Philippon, C., Wastine, B., Rella, C. W., Vuillemin, C., Truong, F., Delmotte, M., Kazan, V., Darding, M., Lebègue, B., Kaiser, C., Xueref-Rémy, I., and Ramonet, M.: Comprehensive laboratory and field

testing of cavity ring-down spectroscopy analyzers measuring H_2O, CO_2, CH_4 and CO, Atmos. Meas. Tech., 8, 3867-3892, https://doi.org/10.5194/amt-8-3867-2015, 2015.

Zellweger, C., Hüglin, C., Klausen, J., Steinbacher, M., Vollmer, M., and Buchmann, B.: Inter-comparison of four different carbon monoxide measurement techniques and evaluation of the long-term carbon monoxide time series of Jungfraujoch, Atmos. Chem. Phys., 9, 3491-3503, 2009.

Zellweger, C., Emmenegger, L., Firdaus, M., Hatakka, J., Heimann, M., Kozlova, E., Spain, T. G., Steinbacher, M., van der Schoot, M. V., and Buchmann, B.: Assessment of recent advances in measurement techniques for atmospheric carbon dioxide and methane observations, Atmos. Meas. Tech., 9, 4737-4757, https://doi.org/10.5194/amt-9-4737-2016, 2016